NASA TECHNICAL NOTE

NASA TN D-6978

NASA TN D-6978

AN ENGINEERING OPTIMIZATION METHOD WITH APPLICATION TO STOL-AIRCRAFT APPROACH AND LANDING TRAJECTORIES

by Heinrich G. Jacob

Ames Research Center
Moffett Field, Calif. 94035

NATIONAL AERONAUTICS AND SPACE ADMINISTRATION • WASHINGTON, D. C. • SEPTEMBER 1972

1. Report No. NASA TN D-6978	2. Government Accession No.	3. Recipient's Catalog No.
4. Title and Subtitle AN ENGINEERING OPTIMIZATION METHOD WITH APPLICATION TO STOL–AIRCRAFT APPROACH AND LANDING TRAJECTORIES		5. Report Date September 1972 6. Performing Organization Code
7. Author(s) Heinrich G. Jacob		8. Performing Organization Report No. A–4323 10. Work Unit No. 135–19–02–04
9. Performing Organization Name and Address Ames Research Center Moffett Field, Calif., 94035		11. Contract or Grant No. 13. Type of Report and Period Covered Technical Note
12. Sponsoring Agency Name and Address National Aeronautics and Space Administration Washington, D. C. 20546		14. Sponsoring Agency Code

15. Supplementary Notes

16. Abstract

An optimization method has been developed that computes the optimal open loop inputs for a dynamical system by observing only its output. The method reduces to static optimization by expressing the inputs as series of functions with parameters to be optimized. Since the method is not concerned with the details of the dynamical system to be optimized, it works for both linear and nonlinear systems. This report explains the method and applies it to optimizing longitudinal landing paths for a STOL aircraft with an augmented wing. Noise, fuel, time, and path deviation minimizations are considered with and without angle of attack, acceleration excursion, flight path, endpoint, and other constraints. The method is easy to learn and easy to use.

17. Key Words (Suggested by Author(s))	18. Distribution Statement
Flight path optimization Aircraft landing V/STOL aircraft Augmentor wing jet STOL	Unclassified - Unlimited

19. Security Classif. (of this report)	20. Security Classif. (of this page)	21. No. of Pages	22. Price*
Unclassified	Unclassified	42	$3.00

* For sale by the National Technical Information Service, Springfield, Virginia 22151

TABLE OF CONTENTS

AN ENGINEERING OPTIMIZATION METHOD WITH APPLICATION TO STOL–AIRCRAFT APPROACH AND LANDING TRAJECTORIES

Heinrich G. Jacob*

Ames Research Center

SUMMARY

An optimization method has been developed that computes the optimal open loop inputs for a dynamical system by observing only its output. The method reduces to static optimization by expressing the inputs as series of functions with parameters to be optimized. Since the method is not concerned with the details of the dynamical system to be optimized, it works for both linear and nonlinear systems. This report explains the method and applies it to optimizing longitudinal landing paths for a STOL aircraft with an augmented wing. Noise, fuel, time, and path deviation minimizations are considered with and without angle of attack, acceleration excursion, flight path, endpoint, and other constraints. The method is easy to learn and easy to use.

INTRODUCTION

This report presents the results of a study of approximately optimum longitudinal landing trajectories for a short takeoff and landing (STOL) aircraft. Since the study was motivated by the desire to understand the character of the trajectories under various criteria, the approximate optimization procedure discussed in this report appeared appropriate.

There are numerous methods for determining optimum open-loop trajectories. Generally, approaches that reduce optimization to a programing problem by parameterizing variables parameterize the states as well as the controls. The method employed in this study, however, parameterizes only the input controls. While the results obtained in this way are also approximate, they are obtained with a minimum of complexity. The approximate method employed in this study, then, is more of an engineering approach. It is neither elegant nor rigorous, but it is easy to use. While it may require more trials on a digital computer than more sophisticated methods, the complete setup, from initiation of the study to its completion, should be considerably shorter.

The procedure is described in two sections. The first describes the operation of the optimization algorithm itself, how to choose directions and step sizes for search, how to optimize along each direction, and how constraints are to be handled. The second section shows what must be done to use the method in the landing problem. It discusses the mathematical model of the aircraft, the performance criteria, the three control variables, and, most importantly, the selection of the set of finite approximations to the optimum control function.

*National Research Council Postdoctoral Research Associate in residence at Ames Research Center.

The final section of the report presents the results of the investigation. The first results concern straight line flight paths, minimum time, minimum fuel, and minimum noise trajectories. Finally, more practical results are obtained after the introduction of supplementary constraints associated with passenger comfort and pilot preference.

THE OPTIMIZATION METHOD

Before the particular problem of optimizing the flight paths is treated, the method of optimization will be described. First, the general idea of the approach will be discussed. Then the particular stages of the process will be considered in a little more detail. The optimization algorithm used in this study will be explained briefly with a more complete description given in an appendix.

Principle of Operation

The usual problem in optimizing the performance of a dynamic system is to find the control function time histories that drive the system so as to minimize some quality criterion. Here the problem is transformed to a static one of parameter optimization by expressing each control function as a finite series of known time functions. The optimal parameters of the series are then determined by an iterative optimization procedure. The type of series and the number of its terms are chosen so that the expected optimal response can be approximated with sufficient precision.

Figure 1 shows the control functions, represented by a set of coefficients, $c_{ij(i)}$ driving the dynamic system. The subscript j(i) indicates that the numbers of coefficients of the different control variables need not be the same. The performance index, PI, evaluates the output of the system in terms of the chosen quality criterion. The evaluation is stored and compared with values previously determined. This comparison triggers a new selection of coefficients in a particular way, and the process is repeated until the performance index ceases to change. Constraints may be considered either by adding penalty functions to the quality criterion or by introducing boundaries directly into the search space over which the nonlinear programing algorithm operates.

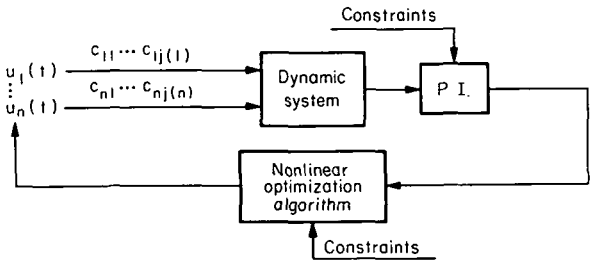

Figure 1.– The optimization procedure.

The type of series expansion chosen to represent the control function is conditioned by any a priori information available on the shape of the optimum functions. If no prior information is available, the simplest series representation to use is the polynomial approximation.

$$u(t) = c_1 + c_2 t + \cdots + c_n t^{n-1} \tag{1}$$

However, because the accuracy of this representation is not uniform in the argument space (ref. 1), such other expansions as trigonometric functions or Legendre polynomials, whose orthogonality properties speed convergence, can also be used. A sine expansion over an interval $[0, T_F]$ takes the form

$$u(t) = c_1 \sin(t\pi/T_F) + \cdots c_n \sin(nt\pi/T_F) \tag{2}$$

To save the computer time required to determine the sine for all n values, equation (2) is written in a trigonometric power series in $R = t\pi/T_F$

$$\begin{aligned} u(t) = {} & c_1[\sin(R)] + c_2[2 \sin(R) \cos(R)] \\ & + c_3[3 \sin(R) - 4 \sin^3(R)] \\ & + \cdots \\ & + c_n\{(n-1) \sin(R) \cos^{n-2}(R) - [(n-1)/3] \sin^3(R) \cos^{n-4}(R) \\ & + [(n-1)/5] \sin^5(R) \cos^{n-6}(R) - \cdots + \cdots\} \end{aligned} \tag{3}$$

Any information available on the shape of the optimal solutions can be used in selecting the approximating functions. An example of useful information is knowledge that the solution switches from one fixed level to another. Then the best choise of coefficients to be found would be the times of occurrence of the levels of control. The choice of switching times as parameters in this case saves computer time and can yield the exact optimal control function (ref. 2).

The performance index is the number computed by evaluation of system output in terms of the quality criterion. Since the number is calculated at each trial of each stage in optimization, the computation should be made rapidly.

Constraints (either equalities or inequalities) may be imposed on the input, output, or internal state variables of the system. If the constraints are inequalities, transition from a permissible to a forbidden region may be gradual or abrupt.

The method of optimization used for this study can handle both types of constraints. For example, the parameters of the control functions are specified at each trial and applied to the system. Each time an inequality constraint violation is detected, the optimization algorithm is signaled to provide a new set of parameters until a set is obtained that violates no boundaries.

Equality constraints, such as terminal constraints on the output, are handled by adding to the quality criterion penalty functions involving the conditions. Since the optimization algorithm involves quadratic functions in an interpolation scheme, the use of quadratic penalty functions is particularly convenient. Penalty functions, of course, may also be used for inequality constraints, especially those where the boundaries are approached gradually.

Constraints imposed on the input functions can sometimes be handled directly by an appropriate choice of type of function for an input. For instance, control functions with switching time as a parameter can easily account for constraints on the number of switches allowed or their minimum time separation.

The Optimization Algorithm

The value of the quality criterion, which is the index of performance of the system for given conditions, is a real valued function of several variables, namely, the parameters of the control function. The object of the optimization algorithm is to start with a given choice of parameters and from there to find the parameters that give an extreme (maximum or minimum) value to the criterion (fig. 2). Several algorithms are available to do this: the one selected should (1) converge quickly to the nearest relative extreme point insensitive to curved valleys and sharp ridges in the parameter-criterion space; (2) permit the imposition of various types of constraints; and (3) be as simple and small as possible to save time for the user and the computer. The algorithm used in this study has these properties: It is simple and short; it appears to be less sensitive to ridges and valleys than other static nongradient methods; and it can handle inequality constraints on the control parameters or their functions. (The Fortran IV program for the algorithm is given in the appendix.)

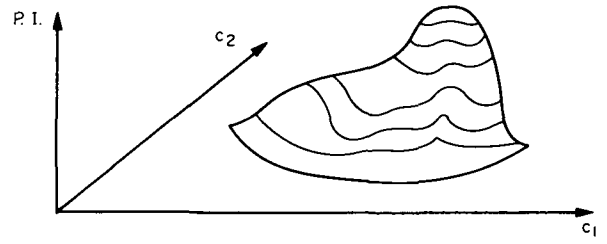

Figure 2.– Performance index as a function of two coefficients.

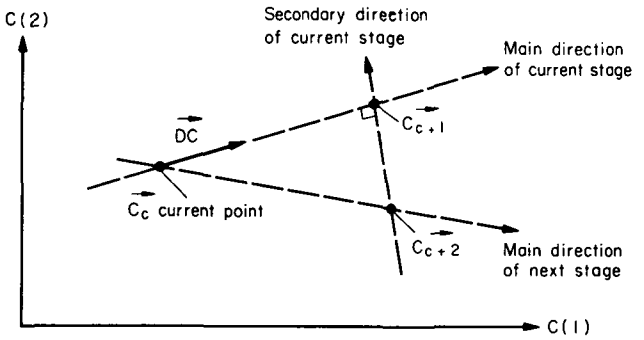

Figure 3.– Determination of the main search direction for a two coefficient problem.

Figures 3 and 4 illustrate the operation of the algorithm in solving the problem of how to change the present or current values of the parameters to improve the performance index. Figure 3 shows a current choice of coefficients C_C as a point in a plane of two parameters C_1 and C_2. This point has been reached from a previous point by a change in the parameter values along the line labeled "main direction of current stage." Before another change is made to point $\overrightarrow{C_{C+2}}$ along the main direction of the next stage, the next main direction must be found by a number of changes along secondary directions as part of the current stage of computation. The number of secondary directions is one less than the number of coefficients to be determined.

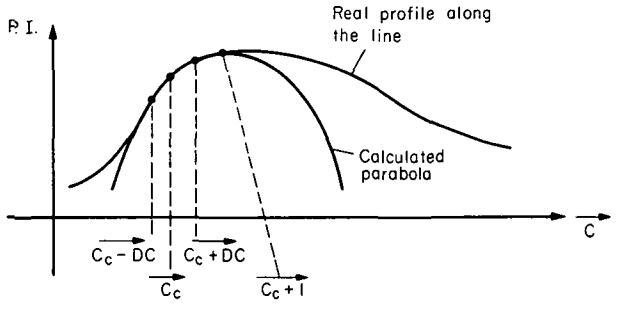

Figure 4.– Extrapolation along a line.

The point $\overrightarrow{C_{C+1}}$ from which the first secondary direction will be drawn is found by changing the coefficients a predetermined amount $\overrightarrow{DC}$ first parallel to the main direction of the current stage, then antiparallel to this direction. The performance index associated with each of the three points $\overrightarrow{C_C - DC}$, $\overrightarrow{C_C}$, and $\overrightarrow{C_C + DC}$ is calculated as illustrated in figure 4, and a parabola is fitted to these three points. At point $\overrightarrow{C_{C+1}}$ in figure 4 the interpolating (or extrapolating) parabola reaches its extreme value. This is the starting point for the first secondary direction, which is orthogonal to the main direction $\overrightarrow{C_C}$,

$\overrightarrow{C_{c+1}}$ as a simple way of guaranteeing that all independent directions in parameter space are tested. This process of finding a starting point and a secondary direction is repeated until the number of main and secondary directions equals the number of (independent) coefficients of the control functions. The final step of this stage of the calculation is to find the point in figure 3 $\overrightarrow{C_{c+2}}$ which is the point of the maximum of the parabola fitted through the performance indices of the three points along the last secondary direction. The direction defined by points $\overrightarrow{C_c}$ and $\overrightarrow{C_{c+2}}$ is the main direction for the next stage of the calculation.

The step size DC is variable during the computations. If any new interpolated point along a line is closer to the old point than one quarter of the current step size along this line, then the current step size will be divided by 4. On the other hand, if the new point is calculated to be farther away from the old point than 20 times the current step size, the step size will be multiplied by 2.

Constraints limiting the evolution of the input, state, and output variables are taken into consideration as follows: Before and during any computation of the performance index, the variables are checked continually to make sure that they lie in the permitted area. As soon as one or several variables violate a boundary, the computer-control flow is given back to the optimization algorithm, which delivers another set of input function coefficients. This process is repeated if necessary until input functions are delivered that do not violate these boundaries.

By means of the search along the continuously corrected optimal direction, the extrapolation or interpolation procedure, and an automatic adjustment of the variable step size DC along each direction, the algorithm converges quickly to the optimum and is able to follow accurately sharp ridges or steep-curved valleys in the coefficient space. (Further details are provided in the appendix.)

From this general description, the dynamic optimization scheme can be seen to have the following characteristics. It is a *direct method* because the cost function is optimized by a direct evaluation of the corresponding quality criterion to index the performance. The optimization is *open loop* in the sense that each new set of initial states of the dynamical system requires a new determination of the optimal control function coefficients. The optimal controls form only an *approximate solution* to the problem since the number of coefficients is limited and the type of series expansion employed may not be the most succinct expression of control possible. The optimization procedure, furthermore, reveals only the *local optimum* nearest the initial set of coefficients. Broader claims for the optimum will necessitate the use of other control function expansions with new coefficients.

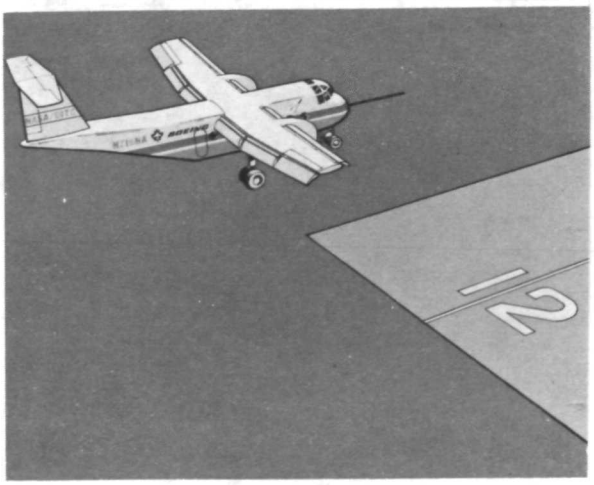

Figure 5.– C–8A augmentor wing STOL aircraft.

ELEMENTS IN FLIGHT PATH OPTIMIZATION

The Aircraft

The augmentor wing STOL vehicle (fig. 5) considered in this study is a modified version of a

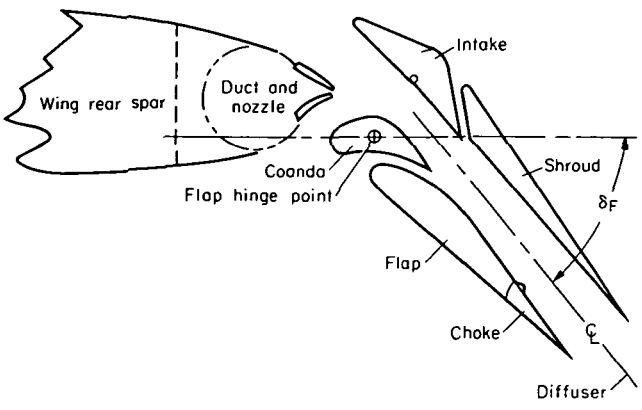

Figure 6.– Augmentor flap arrangement.

C-8 Buffalo aircraft by deHavilland of Canada (ref. 3). The wings and engine were modified to enhance the aircraft's short takeoff and landing capability. The normal lift of the wings was augmented by the addition of a cold air duct and redesign of the flaps. The flaps are in effect a diffuser, and cold air ducted along the wing is exhausted through long nozzles (fig. 6). As the flow of air passes through the diffuser formed by the flap, it induces additional flow through the intake portion of the flap. The cold air flow effects added direct thrust from the throat of the flap and added lift due to increased aerodynamic circulation (ref. 4).

Two Rolls Royce Spey Mk 801 SF jet engines replace the previous turboprop engines. The hot exhaust gas of the engines can be deflected through a total angle of 98° to provide additional lift and braking for the vehicle. The hot thrust vectoring and augmented lift give this vehicle an unusual control capability.

Mathematical Models for Computation

The following simple two-dimensional equations of motion were used to model the aircraft.

$$\dot{u} = X_A - g \sin \theta + \frac{T}{m} \cos \sigma - \dot{\theta} w \tag{4a}$$

$$\dot{w} = Z_A + g \cos \theta - \frac{T}{m} \sin \sigma + \dot{\theta} u \tag{4b}$$

$$\dot{x} = u \cos \theta + w \sin \theta \tag{4c}$$

$$\dot{z} = -u \sin \theta + w \cos \theta \tag{4d}$$

where, with the coordinates defined in figure 7,

$\dot{u}$ acceleration along the body x-axis

$\dot{w}$ acceleration along the body z-axis

$\dot{x}$ horizontal geographical speed

$\dot{z}$ vertical geographical speed

g gravity acceleration 32.1725 ft/sec^2 (9.805 m/sec^2)

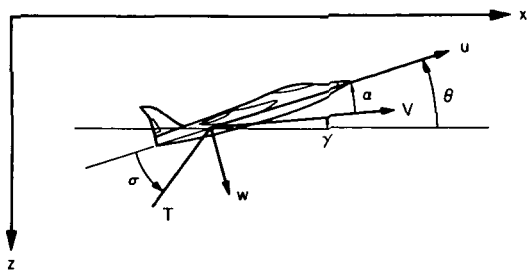

Figure 7.– Coordinate system.

θ pitch angle

σ thrust angle

T hot thrust, lb (N)

m W/g aircraft mass with W = 40,000 lb (17,438 kg)

The forces X_A and Z_A are given in terms of the lift and drag coefficients C_L and C_D and the parameters and variables indicated below.

$$X_A = -C_D(\alpha, C_J, \delta_F)\, q\, \frac{S \cos \alpha}{m} + C_L(\alpha, C_J, \delta_F)\, q\, \frac{S \sin \alpha}{m} \tag{5a}$$

$$Z_A = -C_D(\alpha, C_J, \delta_F)\, q\, \frac{S \sin \alpha}{m} - C_L(\alpha, C_J, \delta_F)\, q\, \frac{S \cos \alpha}{m} \tag{5b}$$

where

$$q = \frac{1}{2}\, \rho V^2$$

and

ρ atmospheric density 0.00238 lb sec^2/ft^4 (1.231 kg/m^3)

V total speed, ft/sec (m/sec)

S reference wing area 865 ft^2 (80.36 m^2)

α angle of attack

γ flight-path angle

δ_F flap angle

C_L $C_L(\alpha, C_J, \delta_F)$, coefficient of lift

C_D $C_D(\alpha, C_J, \delta_F)$, coefficient of drag

C_J $T_C(T)/qS$, cold thrust coefficient

$T_C(T)$ cold thrust, lb, a function of the hot thrust

The control variables in equations (4) are: pitch angle θ; hot exhaust or thrust angle σ; and throttle angle θ_e. The study assumed that the pilot or autopilot could generate θ directly, with no intervening dynamics. The throttle angle θ_e is related to the hot thrust by

$$T = 355.1^\circ\ \theta_e\ (= 1592\ \theta_e, \text{N}) \tag{6}$$

with θ_e given in degrees. The flap setting δ_F is taken to be constant at 75° for this study.

With the above equations all state and output variables of the aircraft, necessary for the determination of the performance index, may be computed, with the exception of the parameters $T_C(T)$, $C_L(\alpha, C_J, \delta_F)$ and $C_D(\alpha, C_J, \delta_F)$ whose values can be obtained from functions fitted to test data. Figure 8 (taken from Boeing Document D6-26065 TN, 1971) shows the hot and cold thrust as a function of the throttle angle. The aerodynamic lift and drag parameters C_L and C_D are shown as a function of angle of attack α and cold thrust coefficient C_J in figure 9; the measured data (denoted by Δ) are also from Boeing Document D6-26065 TN. The cold thrust T_C is given empirically by the following expressions

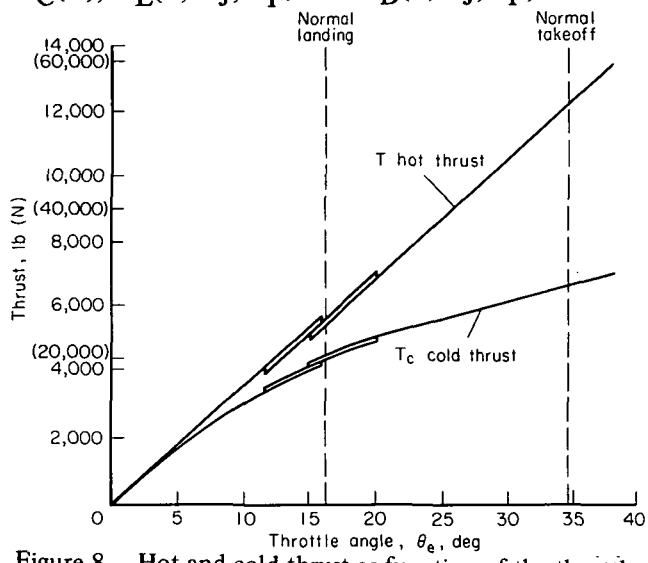

Figure 8.– Hot and cold thrust as function of the throttle angle.

$$T_C = T(1 - 0.0143\,\theta_e) \qquad \theta_e \leq 20^\circ \tag{7a}$$

$$= T(0.2557 + 8.57/\theta_e) \qquad \theta_e > 20^\circ \tag{7b}$$

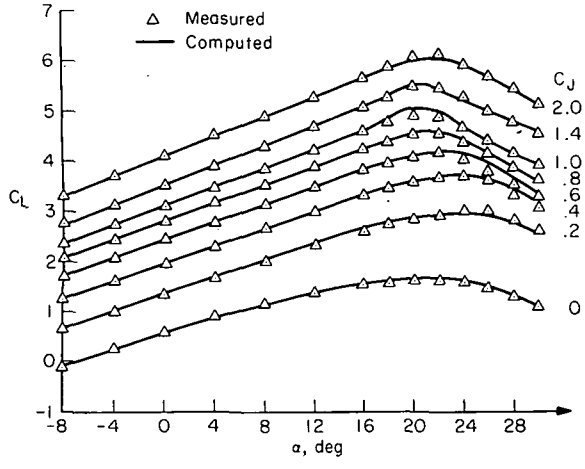

(a) Aerodynamic lift.

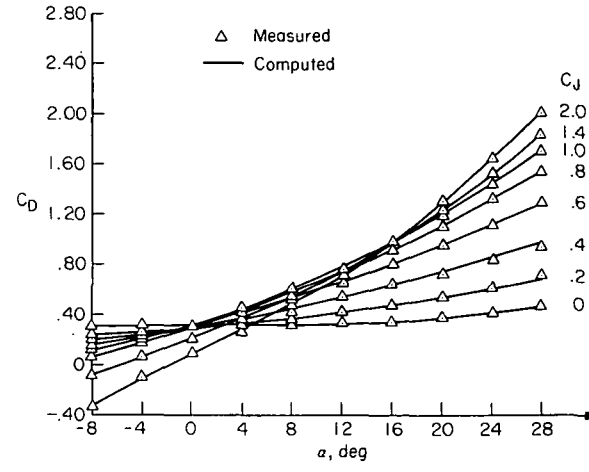

(b) Aerodynamic drag.

Figure 9.– Aerodynamic lift and drag parameters for flap angle $\delta_F = 75^\circ$ and aileron angle $\delta_A = 0^\circ$.

The parameter identification method described in reference 5 was used to give the functional fit shown in figure 9 for C_L and C_D. The functions used for the fit were hyperbolas and polynomials. When coupled with some least squares criterion program, the optimization algorithm described in the appendix could also have been used to fit the data.

After the data shown in figure 9 were obtained, the aircraft design was modified so that the ailerons droop automatically as the flaps are deflected. With the flaps set at 75°, the ailerons droop 30°. This droop has a negligible effect on the drag coefficient, but changes the lift coefficient in the following way:

$$C_L = C_L^* + 0.115 + 0.28\, C_J \tag{8}$$

where C_L and C_L^* are the coefficients with and without droop considered, respectively, for a flap setting of 75°.

A number of control and state constraints were imposed on the problem of determining optimum landing flight paths. Some are physical or hardware constraints, referred to as design constraints, that were taken into account in every calculation: throttle angle, thrust angle, angle of attack, and total flight speed. These constraints are listed in table 1.

Other constraints, referred to as safety and comfort constraints, are concerned with pilot's preference or ride quality (table 2). For some computations of the flight trajectories the controls were changed only at certain times and remained constant otherwise, leaving the pilots free to check other flight parameters. These restrictions on the handling capabilities of the input commands were accounted for by the choice of an appropriate class of possible input functions.

TABLE 1.– DESIGN CONSTRAINTS

Throttle angle, θ_e	$0° \leqslant \theta_e \leqslant 35°$
Thrust angle, σ	$18° \leqslant \sigma \leqslant 116°$
$\dot{\sigma}$	$\lvert\dot{\sigma}\rvert \leqslant 60°/\text{sec}$
Angle of attack, α	$-10° \leqslant \alpha \leqslant 30°$
Forward speed, V	$V \leqslant 95$ knots

TABLE 2.– SAFETY AND COMFORT CONSTRAINTS

Normal acceleration change	$\lvert\Delta a_n\rvert \leqslant 0.15g$
Pitch rate	$\lvert\dot{\theta}\rvert \leqslant 10°/\text{sec}$
Throttle position	$16° \leqslant \theta_e \leqslant 35°$
Angle of attack	$\alpha \leqslant 8°$ (except during flare)

Two different structures were chosen to represent the control variables. The first structure, allowing general unconstrained flight paths, was a modified finite sine series of the form:

$$\theta = c(1,1) + c(1,2)\frac{x}{x_i} + c(1,3)S_R + c(1,4)2S_RC_R + c(1,5)(3S_R - 4S_R^3)$$

$$+ c(1,6)(8S_RC_R^3 - 4S_RC_R) + c(1,7)(16S_RC_R^4 - 12S_RC_R^2 + S_R)$$

$$+ c(1,8)(6S_RC_R^5 - 20S_R^3C_R^3 + 6S_R^5C_R) \tag{9a}$$

$$\sigma = c(2,1) + c(2,2)\frac{x}{-x_i} + \cdots \tag{9b}$$

$$\theta_e = c(3,1) + c(3,2)\frac{x}{-x_i} + \cdots \tag{9c}$$

where c(i,j), i = 1, 3; j = 1, 8, coefficients whose optimal values have to be determined

x geographical horizontal distance in feet (meters) to the touchdown point

x_i initial geographical horizontal distance in feet (meters) to the touchdown point

S_R $\sin(-\pi x/x_i)$

C_R $\cos(-\pi x/x_i)$

Formulas (9a), (9b), and (9c) are derived from equation (3) by adding a constant term and a linear term (ramp), and choosing the geographical horizontal distance x to the touchdown point as the independent variable.

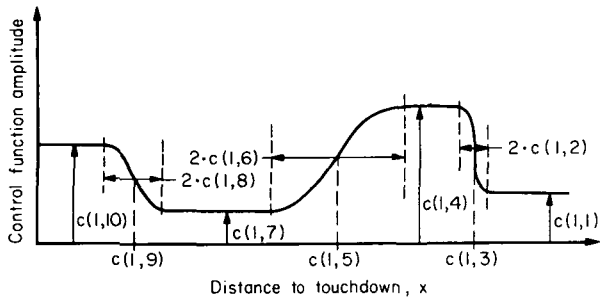

Figure 10.– Structure of input control functions comprising hyperbolic tangent.

As will be seen, the optimal control histories resulting from the sine series for input functions present continuously varying and sometimes oscillating time histories. These are difficult for pilots. To obtain control functions acceptable to pilots the following structure of input functions was selected, which yields control time histories that vary only periodically (fig. 10).

$$\theta = \frac{c(1,1) - c(1,4)}{2}\tanh\frac{2[x - c(1,3)]}{|c(1,2)|} + \frac{c(1,1) + c(1,4)}{2} + \frac{c(1,4) - c(1,7)}{2}\tanh\frac{2[x - c(1,5)]}{|c(1,6)|}$$

$$- \frac{c(1,4) - c(1,7)}{2} + \frac{c(1,7) - c(1,10)}{2}\tanh\frac{2[x - c(1,9)]}{|c(1,8)|} - \frac{c(1,7) - c(1,10)}{2} \tag{10a}$$

$$\sigma = \frac{c(2,1) - c(2,4)}{2} \cdots \tag{10b}$$

$$\theta_e = \frac{c(3,1) - c(3,4)}{2} \cdots \tag{10c}$$

The 10 coefficients of the input control function shown in figure 10 permit three successive flight-path changes. As used in this study, each of the three control functions can have the same amount of freedom, as shown, with the one limitation that all three functions must switch at the same time. If fewer flight-path changes are foreseen, only seven or even four coefficients are necessary for each input control function.

Definition of the Quality Criteria

The following quality criteria were considered for the optimization.

Time minimum– The corresponding performance index for any flight path considered requires simply measuring the time needed to move from the fixed initial point to the desired endpoint.

$$PI = \int_{t_i}^{t_f} dt = T_F \tag{11}$$

Fuel minimum– For this criterion it was assumed that the hot thrust is approximately proportional to the fuel rate.

$$PI = C_F \int_{t_i}^{t_f} T(t)dt = F_F \tag{12}$$

where

T hot thrust in lb (N)

t_i, t_f initial and final flight time; t_f free

C_F 0.22×10^{-3} lb/lb sec (conversion factor)

Noise minimum–From the numerous and complex noise definitions available, an approximate formula was developed to estimate the amount of noise inconvenience encountered by the people living in the community surrounding a STOL airport and by the people in the neighborhood of the runway. The performance index for the minimum noise criterion involves three major factors: the distance function, the expression used for maximum perceived noise, and the modification of the maximum perceived noise expression by which it is converted to the maximum effective perceived noise expression.

In calculating noise, two expressions are used for the distance: the altitude of the airplane from the initial point until the airplane is 1550 ft (472 m) horizontally from the touchdown point; and the slant distance from the airplane to the ground 200 ft (61 m) lateral to the airplane's ground track from the 1550-ft (472 m) point until touchdown. Two expressions are used because STOLports (refs. 6, 7) are considered to have a cleared area beginning at a point about 1550 ft

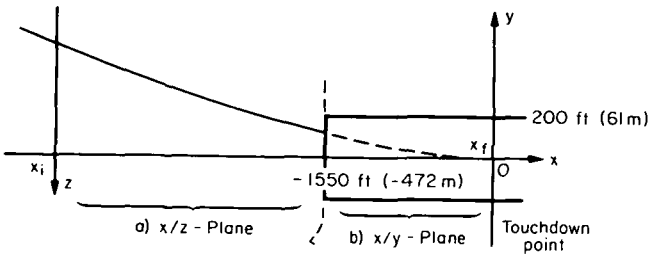

Figure 11.– Noise level estimation.

(472 m) from touchdown; touchdown is assumed to occur 550 ft (168 m) from the beginning of the runway pavement, and the cleared area begins 1000 ft (305 m) from the pavement. The noise is evaluated along a line 200 ft (61 m) away from the centerline of the cleared area. In figure 11 a trajectory in the x-z plane is shown on the left and the line of noise evaluation in the x-y plane on the right. The population density is assumed uniform along the line of evaluation and the same for both distance expressions.

The maximum perceived noise level (MPNdB) may be expressed approximately by (ref. 8):

$$\text{MPNdB} = 123 + 25 \log_{10}(500/D_N) + 52 \log_{10}(T/12{,}200) \tag{13}$$

where 123 is the perceived noise level in dB encountered at a distance of D_N = 500 ft (152 m) from the STOL aircraft flying with a hot thrust of T = 12,200 lb (54,680 N).

The value of MPNdB varies along the flight path with the hot thrust T and the altitude of the aircraft. The distance D_N is measured from the noise source (aircraft) to the closest point along the flight path where people might be. From the previous discussion, this closest distance is taken to be

$$D_N = -z \qquad \text{for } x_i \leqslant x < -1550 \quad (-472)$$

$$D_N = \sqrt{z^2 + 200^2} \qquad \text{for } -1550 \leqslant x \leqslant 0$$

$$\left(\sqrt{z^2 + (61)^2}\right) \qquad (-472 \leqslant x \leqslant 0)$$

where x is the (negative) distance to the desired touchdown point and z is the (negative) altitude, both in ft (m) (fig. 11). The total integral amount of MPNdB along the complete flight path would be

$$\int_{x_i}^{x_f} \text{MPNdB}(x)dx = \int_{t_i}^{t_f} \text{MPNdB}(t)V_x(t)dt(\text{dB ft}) \ (\text{dB m}) \tag{14}$$

where V_x = horizontal speed in ft/sec (m/sec). A time term is added to equation (14) to obtain the duration of the effective perceived noise. The effect of the noise duration on the sensation of people can be approximated by adding 3 to 8 dB (depending on the type of the noise) to the basic PNdB value for each doubling of the noise duration (refs. 9, 10) which yields

$$\text{EPNdB} \approx \text{PNdB} + k \log_{10}(t/t_{ref}) \tag{15}$$

with $10 < k < 27$. In consequence, from expressions (13), (14), and (15) and knowing that the time is inversely proportional to the horizontal speed of the aircraft, one gets for the "integral maximum effective perceived noise" ($\int$MEPNdB·dx) over the total flight path:

$$N_F = \int_{x_i}^{x_f} MEPNdB(x)dx = \int_{t_i}^{t_f} \left\{ MPNdB(t) + k \log_{10}\left[\frac{V_{ref}}{V_x(t)}\right]\right\} V_x(t)dt \qquad (16a)$$

Choosing k = 20 and taking as a reference speed V_{ref} = 60 knots ≈ 101.2 ft/sec (30.85 m/sec) gives the index of performance corresponding to a minimum noise quality criterion

$$PI = \int_{t_i}^{t_f} MEPNdB(t)V_x(t)dt$$

$$= \int_{t_i}^{t_f} \left[MPNdB(t) + 20 \log_{10} \frac{101.2}{V_x(t)} \right] V_x(t)dt = N_F \qquad (16b)$$

This minimized noise performance index N_F has a dimension EPNdB feet (EPNdB meters) that is not very revealing. Hence, the value N_F was divided by the horizontal flight distance to get an average effective noise $\bar{N}_F$ encountered on ground from the initial (x_i) to the final (x_f) flight point:

$$\bar{N}_F = \frac{N_F}{x_f - x_i} \qquad (16c)$$

Deviation minimum— This quality criterion is based on the measurement of the integral absolute error between an actual flight path and a predefined, desired one. The desired path may consist of two straight line parts, for example, the first part of the trajectory might have a flight path angle of $\dot{\gamma} = 0°$ (horizontal flight) and the second part (descent to the aim point), with a flight path angle of $\gamma = -7.5°$. The index of performance corresponding to this criterion is calculated by

$$PI = \int_{x_i}^{x_f} |z - z_d|(x)dx = D_F \qquad (17)$$

where z_d = desired negative altitude at the point x.

Two or more quality criteria— Cases involving two or more quality criterion simultaneously (e.g., deviation minimum and fuel minimum) were also considered during the determination of optimal landing trajectories. The total performance index is then the sum of the squared and differently weighted single performance indices.

RESULTS AND DISCUSSION

The calculations of optimal landing flight paths for the augmentor wing STOL aircraft fall into three general categories. The first contains optimal input controls for straight line flight paths. The second category contains results obtained for optimum landing profiles on the basis of different individual criteria. These profiles are chiefly of theoretical interest. The third category contains more practical results. The control functions are more representative of those a pilot would choose to employ and the constraints are intended to represent those required in practice. This division of

results into theoretical and practical turns out to be somewhat arbitrary, because although the practical results begin with a trajectory with a complete set of constraints, the effects of removing some of them are then evaluated.

Optimum Input Controls for Straight Line Flight Paths

It is possible to determine optimal input controls even for straight line trajectories. Indeed, when fixing both the flight path angle and the speed of the aircraft, there is still one degree of freedom among the three control variables.

Horizontal flight paths— The aircraft is considered to be in equilibrium flying a straight horizontal course with its flaps deflected to 75°. Each control function has only a single parameter to be optimized for given quality criteria: pitch angle $\theta = c(1,1)$, thrust angle $\sigma = c(2,1)$, and throttle angle $\theta_e = c(3,1)$. Results are shown in figure 12 where the abscissa gives the forward speed in knots, and the ordinate gives the controls θ, σ, and θ_e for minimum fuel and noise, the state (α), the fuel required (F_F), and the average noise ($\overline{N}_F$) above 70 dB produced at an altitude of 700 ft (214 m) above ground for 1.0 n.mi. (1.85 km). The solid lines show the values determined with a maximum angle of attack $\alpha = 8°$; the broken lines were obtained without this restriction.

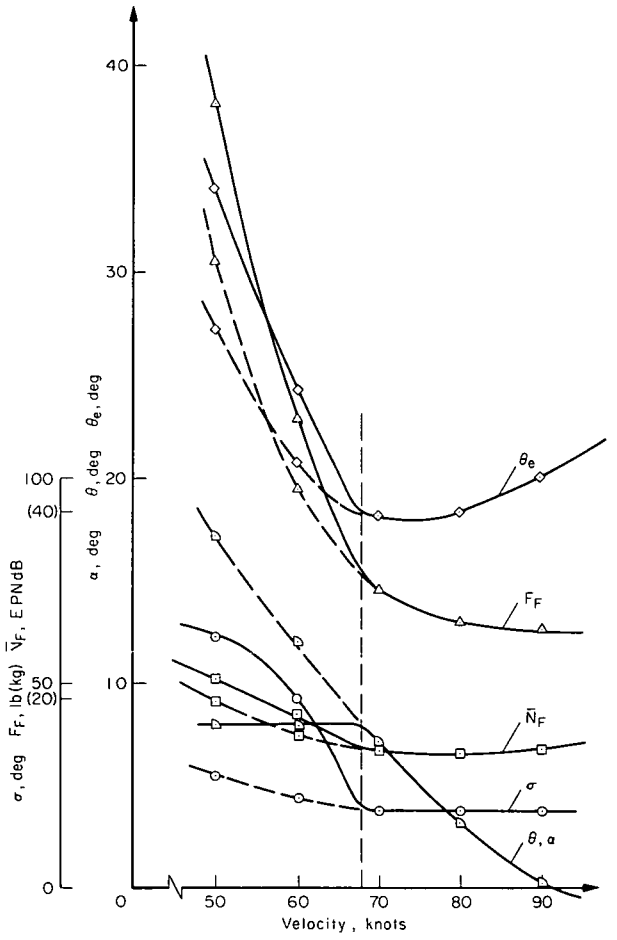

Figure 12.— Fuel and noise minimum horizontal flight ($\delta_F = 75°$).

For a fixed speed, the indicated values correspond to both a horizontal *minimum fuel* flight from one given point to another, and to a horizontal *minimum noise* flight because when the altitude and the speed are fixed, noise depends only on the magnitude of the thrust. As an example of typical control settings, in horizontal equilibrium flight at V = 80 knots, figure 12 gives $\theta = 3.19°$, $\sigma = 18.58°$, and $\theta_e = 18.34°$.

Figure 12 also shows that a speed of about 90 knots would result in a minimum fuel flight, and a speed of about 80 knots would result in a minimum noise flight.

Descent along a constant 7.5° glide slope– For a straight line descent along a given flight path at a given total speed, one degree of freedom remains for adjusting the three control variables (flap angle = 75°). Figure 13 shows these technically possible combinations of the control positions θ, σ, and θ_e for $\gamma = -7.5°$ and V = 60 knots, with the resulting values of the consumed fuel and effective perceived noise when flying from an initial point $(x_i;z_i) = (-5414$ ft $(-1650$ m); -700 ft $(-214$ m)) to the aim point $(x_f;z_f) = (-100$ ft $(-31$ m); 0). Theoretically it may be feasible to fly with a throttle angle of $\theta_e = 10°$ and corresponding $\theta = 14.76°$ and $\sigma = 34.63°$. The resulting fuel consumption would be 41.8 lb (18.2 kg) and the average noise 98.7 EPNdB.

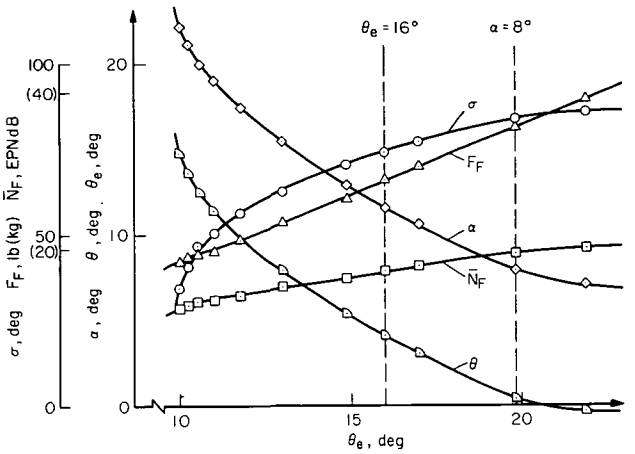

Figure 13.– Inputs and states as a function of the throttle angle θ_e for $\gamma = -7.5°$ and V = 60 knots.

Although this adjustment of the controls is advantageous with regard to the fuel and noise criteria, the safety constraints of $\theta_e \geqslant 16°$ and $\alpha \leqslant 8°$ are not met. The α requirement is the more stringent and to meet it, one has to adjust input controls as follows: $\theta_e = 19.82°$, $\theta = 0.42°$, and $\sigma = 83.75°$ (fig. 13). As shown, the fuel requirement has now nearly doubled to $F_F = 81.7$ lb (35.6 kg) and the noise has increased to $N_F = 114.3$ EPNdB, demonstrating the unfavorable effect on fuel consumption and noise propagation of the limits on the minimum throttle angle and maximum angle of attack.

For a flight path angle of $\gamma = -7.5°$, the fuel and noise optimal controls can be determined from figure 14, for any total speed 50 knots $\leqslant$ V $\leqslant$ 90 knots. Figure 14(a) shows the values when no restrictions are imposed on θ_e and α. Figure 14(b) shows how the controls have to be adjusted when the constraints are considered. It is apparent that for low speed the constraint on angle of attack $\alpha = 8°$ results in an increase of fuel and noise, and for high speed the constraint of a minimum throttle angle $\theta_e = 16°$ causes similar increases.

If the constraints are taken into account, the least fuel and noise figures are obtained at approximately 90 knots. In the case of V = 60 knots, it is apparent that when the constraints are included the fuel usage increases from 41.8 (18.2) to 81.7 lb (35.6 kg) and the average noise from 98.7 to 114.3 EPNdB (the figure shows the value above 70 dB).

Theoretical Optimum Landing Profiles

For the determination of the controls and landing trajectories optimized with respect to noise, fuel, or time, the modified sine series (eqs. 9(a-c)) with eight coefficients for each input variable was chosen. The noise, fuel, or time during the whole trajectory from $(x_i;z_i) = (-1.5$ n.mi. (2.8 km); -700 ft (214 m)) to $(x_f;z_f) = (0;0)$ was integrated using equations (11), (12), or (16b), as appropriate.

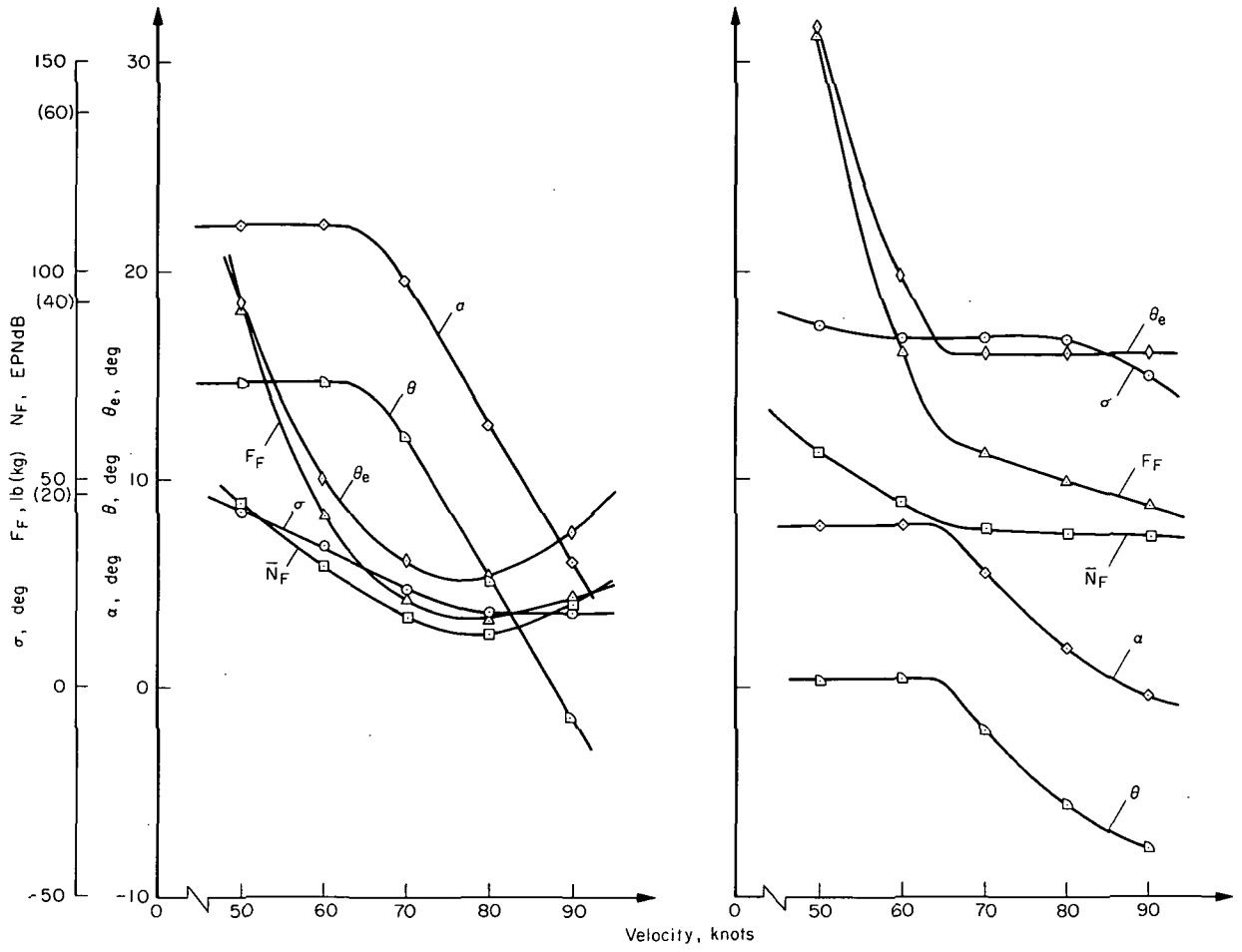

(a) Without safety constraints.

(b) With safety constraints on α and θ_e.

Figure 14.– Fuel and noise minimal flight with $\gamma = -7.5°$ ($\delta_F = 75°$).

So that the aircraft might land at the desired touchdown point with the desired speeds $(V_f;\dot{z}_f)$ = (55 knots; 3 ft/sec (0.9 m/sec)), the applicable performance criterion was augmented by a penalty function involving the weighted quadratic errors of the landing requirements. At the initial point the aircraft is assumed to fly in equilibrium with a horizontal speed of 80 knots and with the values of the controls indicated in figure 12. All the design limitations in table 1 were taken into consideration, but not the safety and comfort constraints in table 2.

Noise minimum landing controls and flight paths–Figure 15 shows the best result of several optimization runs; there are numerous local optima since the problem is highly nonlinear.

Looking at altitude as a function of the distance to the runway, it appears that the aircraft climbs from the initial 700 ft (214 m) to 875 ft (267 m). The thrust magnitude is highest during the

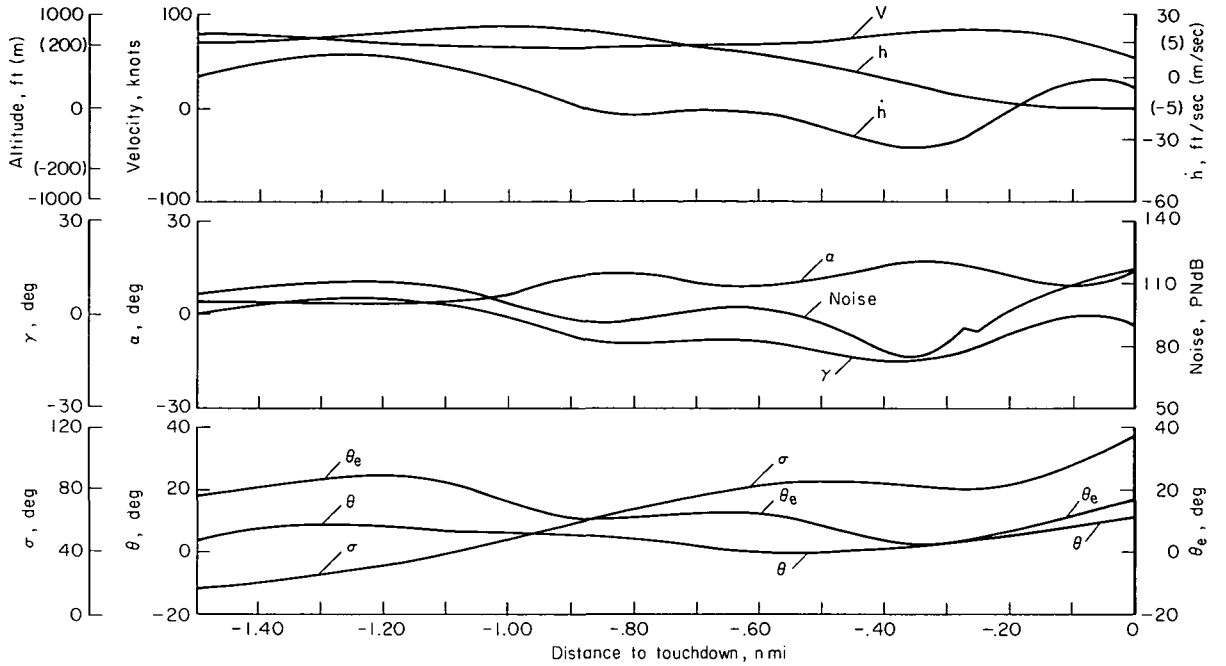

Figure 15.– Minimum noise landing trajectory with design and touchdown constraints only.

first part of the flight. Thus it is profitable to fly as long as possible at the highest possible altitude, since the noise decreases as the distance to the noise source increases. During the middle part of the trajectory the thrust magnitude and corresponding noise level are very low (θ_e going below 3°), the maximum perceived noise decreasing to 72 PNdB. At the end of the flight, however, the thrust has to be raised again to meet the touchdown requirements. For this reason, and partly because the distance of the aircraft to the ground is diminishing, the noise increases during the last part of the trajectory. The noise level drops sharply at x = −1550 ft (−472 m), the beginning of the clear zone in figure 11.

Note that the angle of attack is relatively high during the whole flight (up to 17°); it is more advantageous to get the necessary lift from a higher angle of attack than from a higher magnitude thrust.

The average maximum effective perceived noise along this minimum noise flight trajectory is $\overline{N}$ = 96.7 EPNdB, the fuel consumption is F_F = 81.5 lb (35.5 kg), and the time needed to cover this 1.5 n.mi. (2.8 km) flight path is T_F = 76.0 sec.

Minimum fuel landing–The best minimun fuel controls and corresponding trajectories found are shown in figure 16. The thrust magnitude is extremely low at the beginning of the flight and the aircraft loses altitude quickly. For the remaining part of the trajectory the aircraft has to be pushed with a medium thrust to keep altitude and meet the final touchdown requirements. The average noise increases to $\overline{N}_F$ = 103.4 EPNdB, while the fuel consumed is only F_F = 60.0 lb (26 kg) and the flight time decreases to T_F = 69.7 sec.

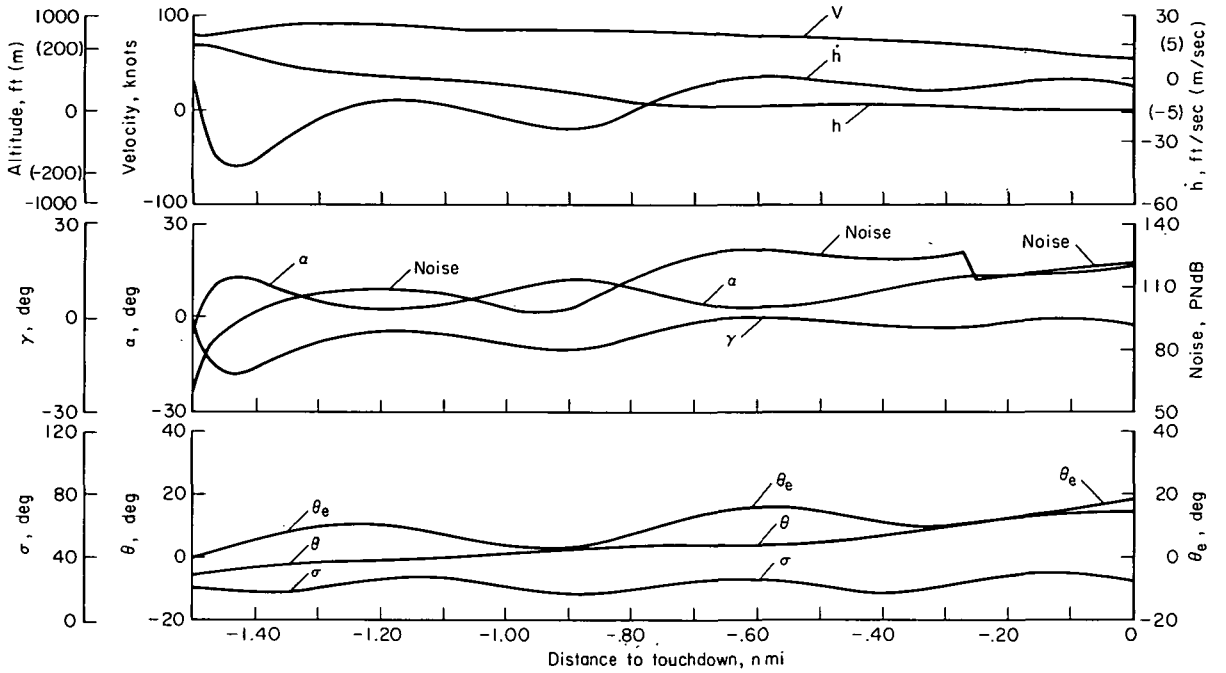

Figure 16.– Minimum fuel landing trajectory with design and touchdown constraints only.

Minimum time landing–Whereas the noise minimal flight path showed at first a climb and the fuel minimal trajectory a dive, the time minimal flight path is nearly straight from the initial to the touchdown point (fig. 17). The thrust magnitude is very high over nearly the complete path to

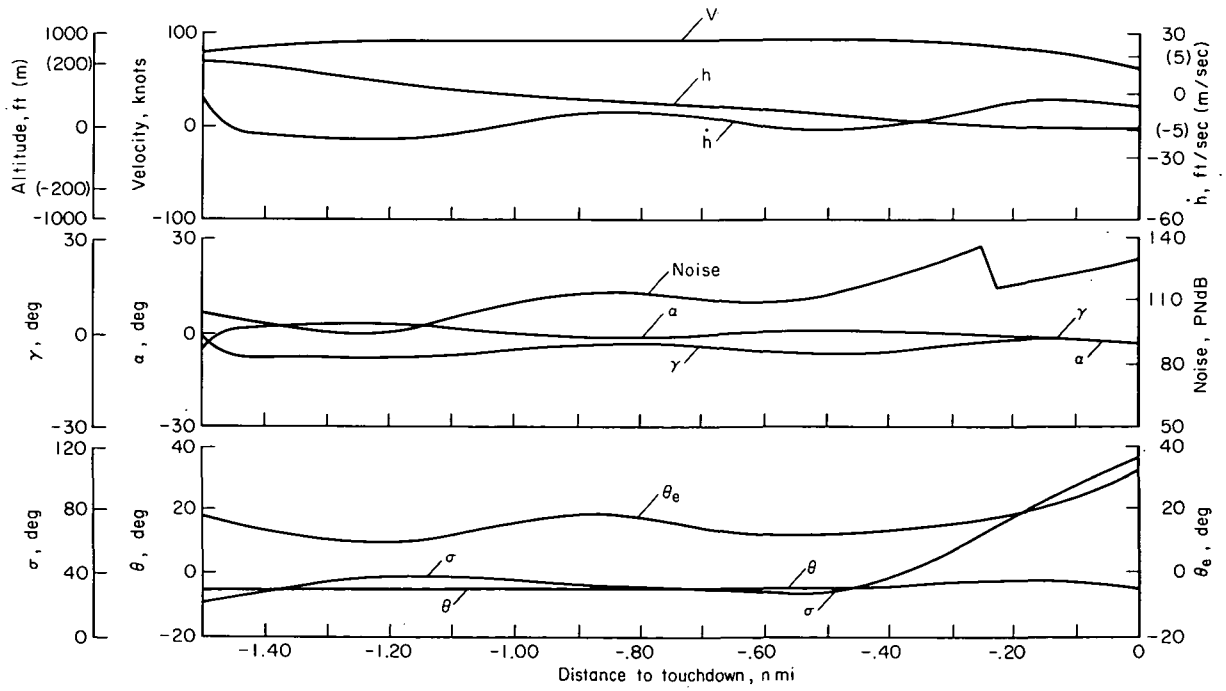

Figure 17.– Minimum time landing trajectory with design and touchdown constraints only.

allow the aircraft to fly with the maximum permitted speed of V_{max} = 95 knots (for $\delta_F = 75°$) at first and then to decelerate to reach an admissible touchdown speed. This reduction is performed by a thrust reversal (i.e., the thrust angle changes from approximately 22° to nearly 116°, the maximum allowable thrust angle). Another characteristic element of this trajectory worth mentioning is that a negative pitch angle is necessary during the entire flight. The greater thrust magnitude causes an increase both in speed and in lift. To allow the aircraft to lose altitude, one has to diminish the angle of attack by a negative pitch angle, particularly at landing when a throttle setting of $\theta_e \cong 34°$ combined with a thrust angle of nearly 116° causes high lift.

For this minimum time flight the resulting average noise is $\bar{N}_F$ = 108.9 EPNdB, the fuel required is F_F = 78.5 lb (34.2 kg) and the flight time is only T_F = 60.6 sec. In achieving these values, however, the optimization procedure for minimum time drove the system to a touchdown speed of 63.6 knots compared to the required speed of approximately 55 knots. This higher touchdown speed is nevertheless low enough to allow a proper landing on a 2000-ft (610 m) STOL runway (ref. 4).

Recapitulation—Figure 18 shows the h/x trajectories obtained for noise, fuel, and time minimum flights, with corresponding values of the average noise produced, fuel required, and the time needed for these flights.

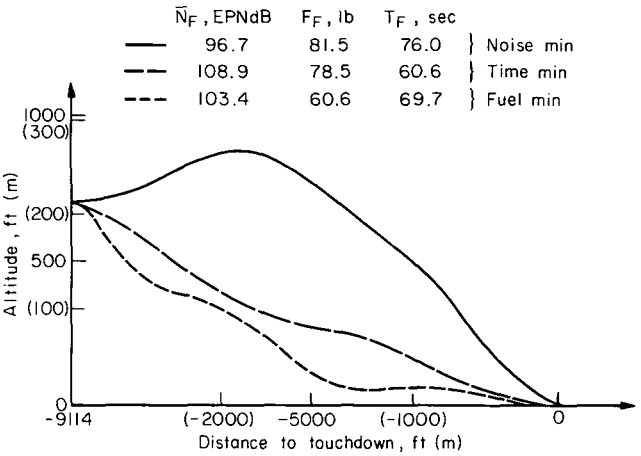

Figure 18.– Landing trajectories without safety and comfort constraints.

Optimum Landing Profiles With Realistic Constraints

We have treated optimum flight paths considering only the design constraints of table 1 and touchdown conditions. In this section, profiles discussed include the constraints and conditions noted, as well as the safety and comfort constraints of table 2 and a height limit at a point 350 ft (107 m) from touchdown. Five landing paths are treated. The first, satisfying all the constraints, will serve as a standard of comparison for the others. In the following trajectories, the effect on noise, fuel, and time of relaxing various constraints will be examined. Before examining these results, however, the height constraint and the control function structure must be explained.

The height constraint will be explained in connection with the following discussion of the nominal landing flight. The nominal conditions are illustrated in figure 19. The aircraft starts in equilibrium at $(x_i;z_i)$ = (−1.5 n.mi. (−2.8 km)/−700 ft (−214 m)) with a speed of

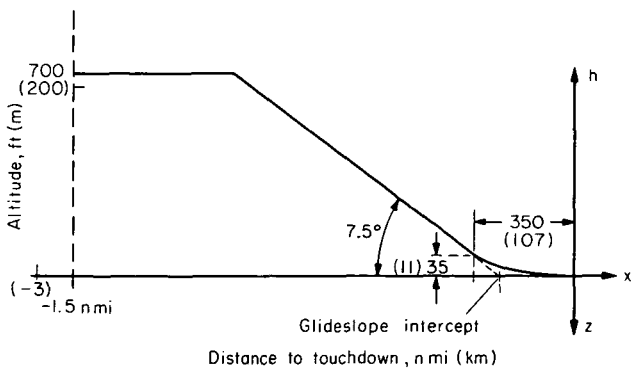

Figure 19.– Desired landing flight trajectory.

$V_i = 80$ knots, $\gamma_i = 0°$ and flap angle constant at $\delta_F = 75°$ during the flight. It flies horizontally with a speed of 80 knots until its flight path crosses a fixed $-7.5°$ glide slope. Then the total speed should be reduced to 60 knots, and the flight path has to follow as closely as possible the $\gamma = -7.5°$ glide slope until a point located at $(x_b;z_b) = (-350$ ft $(-107$ m$)/-35$ ft $(-11$ m$))$ is reached. At this point the total airspeed should still be $V_b = 60$ knots and the vertical speed is expected to be $\dot{z}_b = 13.22$ ft/sec (4.03 m/sec), corresponding to the flight path angle of $\gamma = -7.5°$. Finally, a flare is necessary, allowing a touchdown at $(x_f;z_f) = (0;0)$ with desired speeds of $V_f = 55$ knots and $\dot{z}_f = 3$ ft/sec (0.9 m/sec). To this nominal path we add the limitations on the control variables $(\sigma_{max}, \sigma_{min}, |\dot{\sigma}|_{max}, \theta_{e_{max}}, \theta_{e_{min}})$, the constraints on the states (α_{max}, V_{max}) and the constraints due to the comfort requirements of the passengers $(|V|_{max}, |\dot{\theta}|_{max})$ given in tables 1 and 2.

A control-function structure was selected involving hyperbolic tangents as in equations (12a, b, and c) and illustrated in figure 10. These formulas sometimes involved four trajectory portions (three flight-path changes) and sometimes only three (two changes). The lengths and the centers of the switching intervals were taken to be the same for all three control functions. If a structure with three trajectory portions was chosen, two coefficients defined the center of the switching intervals, two more defined the length of these common switching intervals and 3X3 coefficients defined the amplitude of the steady state portions of the three input functions. Thus, the state optimization algorithm had to determine only the optimal values of 13 coefficients. When four trajectory portions were chosen, 3 + 3 + (3X4) = 18 coefficients had to be optimized.

Fully constrained minimum noise landing flight path—When one sets all the limits in the optimization program and selects a quality criterion comprising a "noise minimum" plus a "deviation minimum" form, so that the flight remains as close as possible to the path specified on figure 19, the optimization procedure delivers the time histories of the inputs, states and outputs indicated in figure 20. (With the trajectory and speeds fixed, the minimum noise and minimum fuel

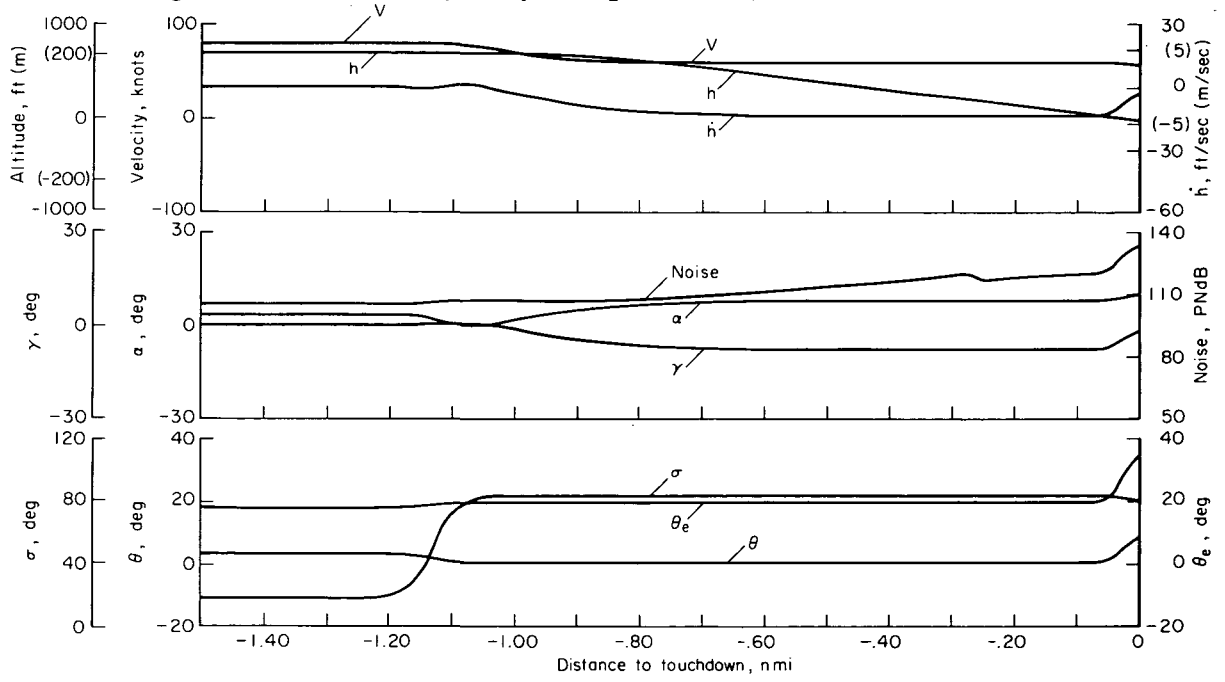

Figure 20.– Minimum noise landing controls and states involving all constraints.

controls are identical.) These results were obtained with input functions involving only three trajectory portions (horizontal 80 knot flight, −7.5° descent at 60 knots, and flare). Note that during the first part of the flight the aircraft is effectively flying with the desired horizontal speed (V = 80 knots, $\gamma = 0°$), with application of the optimal controls ($\theta = 3.19$, $\sigma = 18.58$, $\theta_e = 18.34$) which are the same as those shown in figure 12.

After a maneuver – performed so as to avoid violating the imposed technical and comfort constraints – the aircraft captures the second part of the trajectory, a flight path with $\gamma = -7.5°$ and V = 60 knots. Again the controls encountered ($\theta = 0.45$, $\sigma = 83.74$, $\theta_e = 19.81$) correspond to the controls discussed in connection with optimal straight-line flight paths (see fig. 14(b)). Note that the angle of attack is 7.97°, very close to the limit. At the "flare initiation point" the aircraft is 0.1 ft (0.03 m) lower than the required altitude of 35 ft (11 m) and the effective speeds at this point are V = 59.98 knots and $\dot{z}$ = 12.89 ft/sec (3.93 m/sec), which are nearly the desired speeds.

The third and last part of this trajectory is the flare. With a nose up position, the aircraft touches down at $x_f; z_f$ = 0.04 ft (0.01 m)/−0.08 ft (−0.02 m) with the speeds of V_f = 57.18 knots and $\dot{z}_f$ = 2.98 ft/sec (0.91 m/sec), values that are again very close to the desired numbers.

The average noise produced for this flight involving all constraints is $\overline{N}_F$ = 110.0 EPNdB, the fuel consumed is F_F = 128 lb (56 kg) and the required time is T_F = 82.3 sec.

Landing path with higher descent speed–A descent speed of 60 knots with a flight path angle of $\gamma = -7.5°$, giving a vertical speed of $\dot{z}$ = 13.22 ft/sec (4.03 m/sec), is considered standard for a STOL aircraft landing trajectory. In figure 21, however, the optimal controls and corresponding

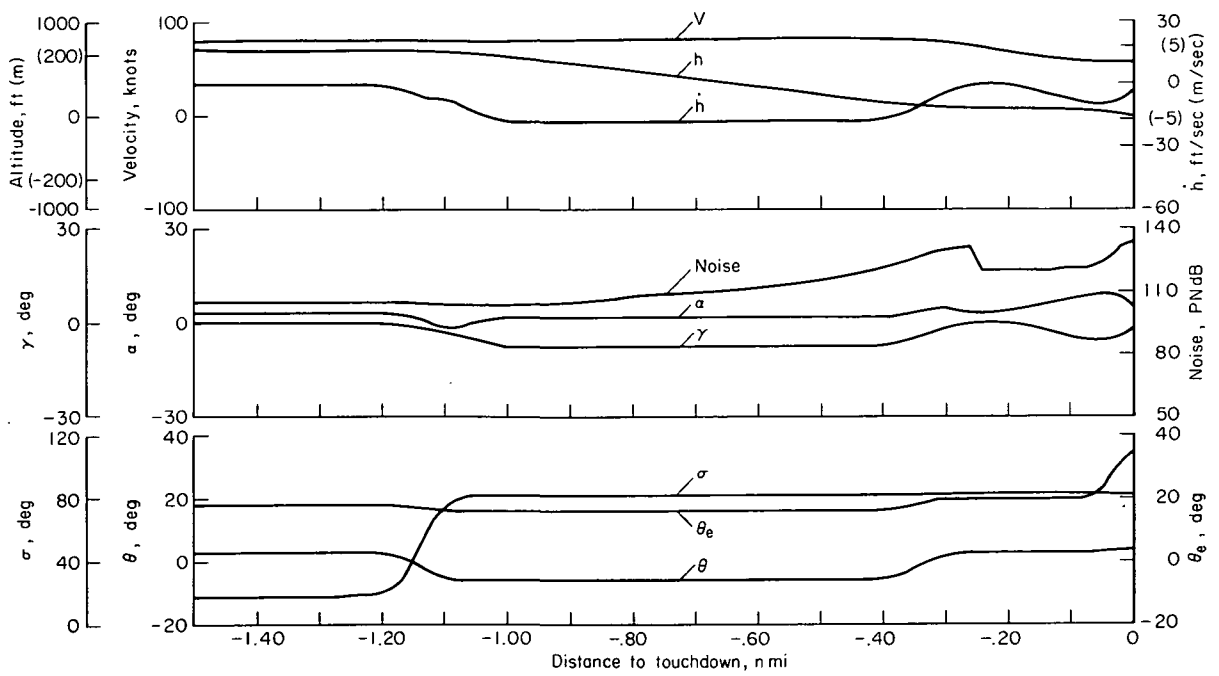

Figure 21.– Controls and states corresponding to a higher descent speed.

states are shown for a flight path angle of $\gamma = -7.5°$ with the higher descent speed of V = 80 knots and vertical speed of $\dot{z}$ = 17.62 ft/sec (5.37 m/sec). Here, the input control functions are divided in four portions: horizontal 80-knot flight, $-7.5°$ flight path at 80 knots, switching to 60 knots, and flare.

The resulting main differences compared to the basic fully constrained trajectory are:

1. Descent speed increased to about 80 knots

2. Angle of attack during the descent much lower with α around 2°

3. A momentary leveling off when the controls change to reduce the speed before touchdown

The average noise resulting from the increased descent speed is slightly lower than for the basic trajectory with $\overline{N}_F$ = 109.4 EPNdB. The fuel consumed decreases to F_F = 101.8 lb (44.4 kg) and the required time is smaller with T_F = 71.0 sec.

Landing path with a higher angle of attack–For adequate stall margin against vertical gusts it is reasonable not to permit descent with an angle of attack greater than 8°. This safety requirement has a strong influence on the noise and fuel characteristics, however (cf. figs. 20 and 22). The results shown in figure 22 required input functions involving only three trajectory portions.

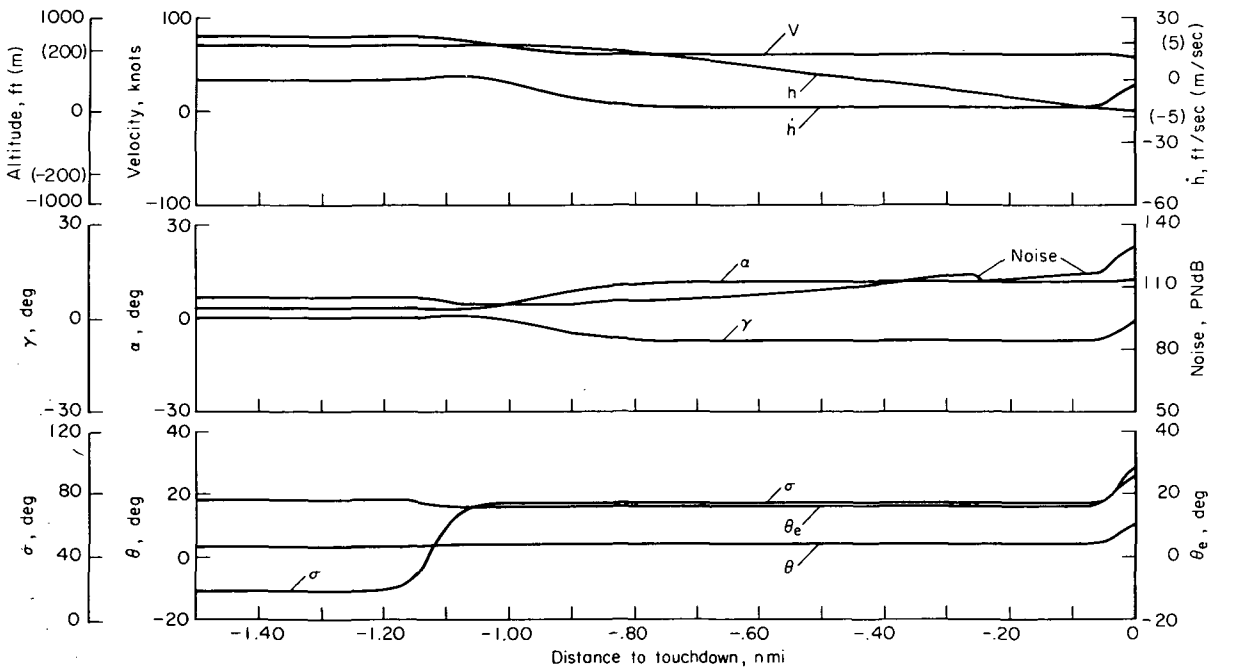

Figure 22.– Controls and states corresponding to a landing with a higher maximum angle of attack.

The controls and states in figure 22 are substantially the same as those in the basic fully constrained trajectory except for the angle of attack (and the associated controls), which increases to nearly 12°. The resulting noise, however, is 3.6 dB lower ($\overline{N}_F$ = 106.4 EPNdB) the fuel is 15.3 percent lower (F_F = 108.5 lb) (47.3 kg) and the time is practically the same (T_F = 82.5 sec).

Landing path with a higher descent speed, steeper flight path angle, and a lower throttle angle– In the example of figure 23, three constraints are relaxed: The descent speed is allowed to go up around 80 knots; the flight path angle, with $\gamma \cong -10°$, is steeper than the recommended $-7.5°$; and the throttle angle is allowed to go nearly as low as 8°.

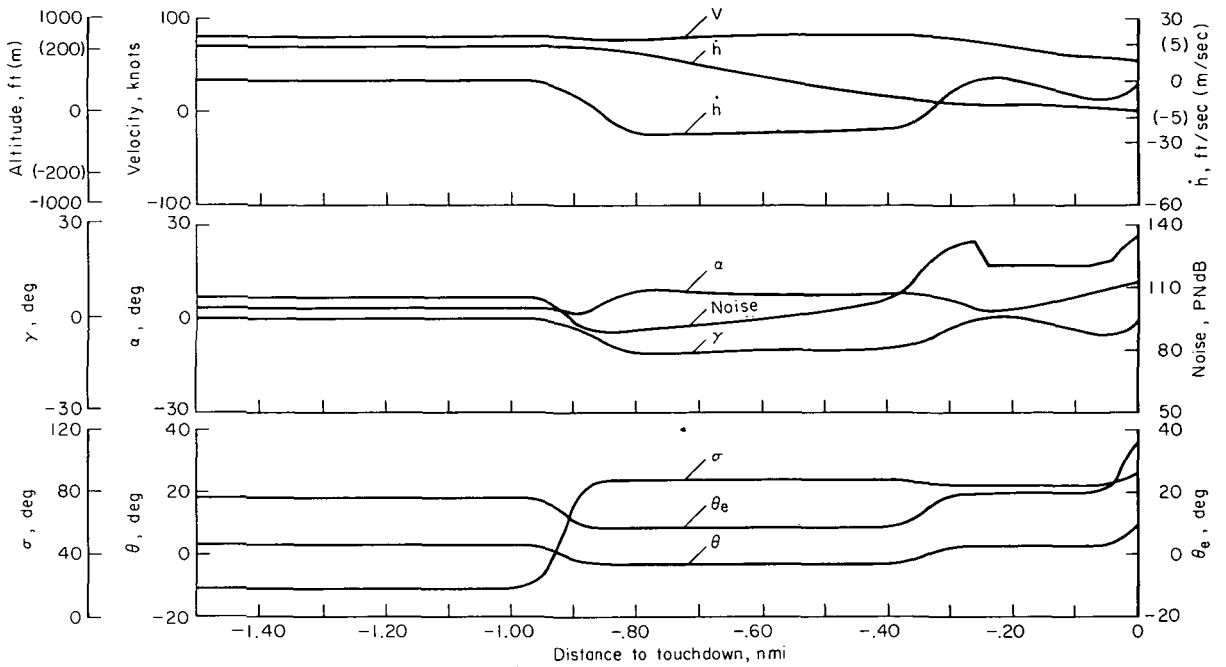

Figure 23.– Controls and states corresponding to a higher descent speed, a steeper flight path angle, and a lower throttle angle.

For this trajectory, the input functions required four portions. The results shown in figure 23 exhibit two main differences from the basic flight path (fig. 20): the aircraft momentarily levels off when changing controls to reduce speed before touchdown, and altitude at inception of flare is only 33.0 ft (10 m), rather than 35 ft (11 m). With the three constraints relaxed, $\overline{N}_F$ is a very low 102.8 EPNdB, $\overline{F}_F$ = 86.0 lb (37.5 kg) and T_F = 70.8 sec.

Landing path with limited constraints–The final minimum noise landing path considered in this investigation was subject only to the constraints of table 1 and an initial horizontal speed of 80 knots, which is maintained up to the point of intercepting the glide slope. The input functions were again divided into four portions. The results (fig. 24) differ significantly in several respects from those for the basic trajectory (fig. 20). Forward speed during descent is 80 knots rather than the nominal 60 knots, the flight path angle steepens to $-11°$ instead of $-7.5°$ and the angle of attack to 20° instead of 8°, and the throttle angle is reduced from 16° to 4.5°. Conditions at the nominal 35-ft (11 m) point are violated: Altitude is 73.4 ft (22.4 m) rather than 35 ft (11 m); the speed is 72.1 knots; and the sink rate is 22.1 ft/sec (6.74 m/sec), nearly twice the nominal value. Finally, the touchdown speed is also high – 70.2 knots instead of the nominal 55 knots – which still is satisfactory for landing on a 2000 ft (610 m) runway (ref. 4).

By integrating the noise developed along this bold landing trajectory and taking its average, one obtains $\overline{N}_F$ = 95.6 EPNdB, 14.4 dB lower than the basic trajectory value of

N_F = 110.0 EPNdB;[1] the fuel consumed F_F becomes 70.6 lb (30.8 kg) (44.8 percent less than the basic trajectory value) and the flight time T_F is 69.1 sec, minus 13.2 sec lower than the basic value.

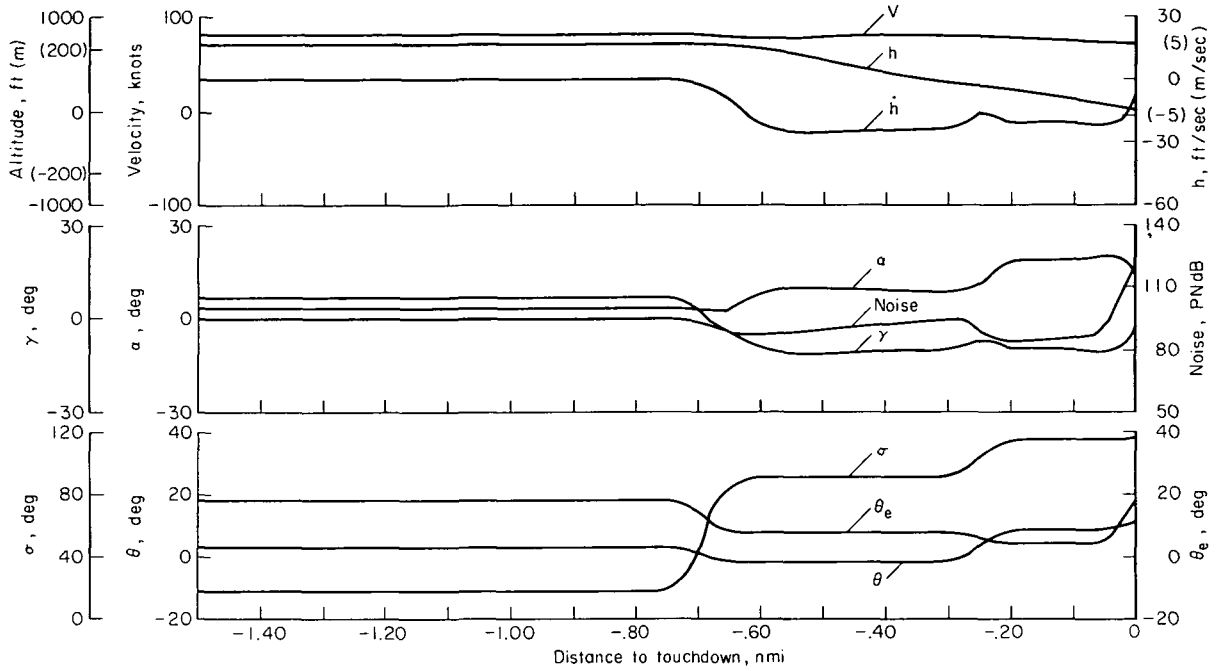

Figure 24.– Controls and states when considering limited constraints.

Recapitulation–Figure 25 summarizes the results of the five cases described in this section. The main characteristics of the different landing flights are specified on the left and the resulting average noise produced, the fuel consumed, the time required, and the change in noise, fuel, and time from the basic trajectory are shown on the right.

Computational Requirements for Optimization of the Flight Paths

The entire Fortran IV computer program consists of four decks. The first, or main, deck, which comprises 80 cards, permits card reading, definition of the input data, and data printout. The data may be: constants, the variable characteristics of the aircraft, given initial and desired final values of the trajectory to be optimized, initial guesses for the control function coefficients, and others.

The computational flow is then directed to the second program, the static optimization algorithm EXTREM, described in the appendix, with 100 Fortran statements.

[1]This average noise produced is lower than the value of N_F= 96.7 EPNdB encountered during the determination of noise minimal landing flights with the use of sine-series input functions (cf. fig. 15). In that investigation the safety and comfort constraints were not considered, but the touchdown requirements nevertheless were met: namely, the speed was held at a low level with V_f = 54.5 knots, whereas, here the touchdown speed is allowed to be very much higher with V_f = 70.2 knots.

After each specification of a new set of input coefficients, the subroutine EXTREM calls a third program, which evaluates the appropriate performance index. To do this the trajectory has to be integrated from the initial to the final point. The noise, fuel, time, and flight path deviations are evaluated at each point along the trajectory and summed. The actual performance index is one or a weighted combination of these quality criteria. This Fortran subroutine permits the selection of the Adams-Moulton, Runge-Kutta, or Euler methods for integration and allows the evolution of the inputs, states, and outputs to be printed out and stored on disk. It comprises nearly 200 cards.

The final program is called by the third program at each integration step. Here the input values of θ, σ, and θ_e are determined from equations (9a-c) or (10a-c). It also evaluates the lift and drag coefficients (figs. 9(a,b)) corresponding to the current state of the aircraft and delivers the derivatives $\dot{u}$, $\dot{w}$, $\dot{x}$, and $\dot{z}$ (eqs. (4a-d)) needed for the flight path integration. This fourth program, which includes 11 different structures for input functions, consists of 120 Fortran statements.

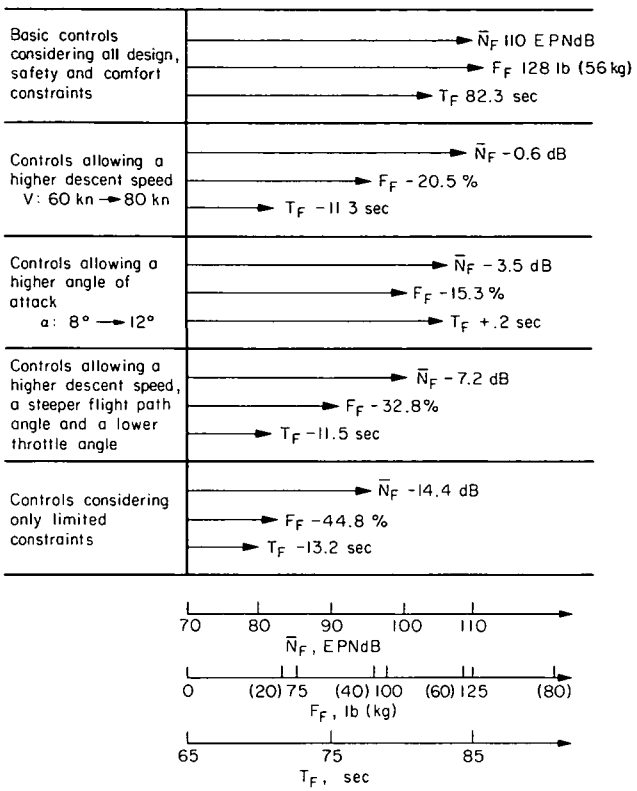

Figure 25.– Effects of constraints on noise, fuel, and time characteristics of a landing trajectory. (In the last four cases, values of $\bar{N}_F$, F_F, and T_F given are differences from those of the basic trajectory.)

Using single precision, the entire program of the four decks, with a total of about 500 cards, requires a storage capacity of 4220 hexadecimal bytes on the IBM 360/67 computer Operating System (OS). The storage requirements associated with the number of coefficients to be optimized is K(K+5) words where K is the number of coefficients.

The computation time necessary for one optimization run depends on the complexity of the problem, the number and type of constraints involved, the number of coefficients to be optimized, and the choice of initial values of these coefficients. Disregarding its dependence on the structure of the control functions and on the choice of initial values, the time of computation increases roughly as the square of the number of input coefficients to be optimized.

The problem of the optimum fuel flight path with design constraints only (fig. 16) can be used as an example of the time required for finding an optimum. The following initial values were used for coefficients of the functions given in equation (9):

c(1,1) = 16 ; c(1,2) = 2.0 ; c(1,3) = · · · c(1,8) = 0

c(2,1) = 26 ; c(2,2) = 3.0 ; c(2,3) = · · · c(2,8) = 0

c(3,1) = 20; c(3,2) = 18 ; c(3,3) = · · · c(3,8) = 0

The initial search step size chosen for all 24 coefficients was |DC| = 1. Convergence with reasonable precision to the final trajectories shown in figure 16 took 7 stages (see appendix) or about 600 trials. One trial corresponds to the integration of one complete trajectory, or one evaluation of the performance index, which is equivalent. This optimization run requires about 5 min using Euler integration with a step size of $\Delta t = 1.0$ sec.

CONCLUSIONS

An engineering dynamic optimization method was described that requires access only to the inputs and the output of the system whose performance is to be optimized. The method consists in transforming the dynamic problem into a static one by representing the input controls as analytical functions whose coefficients have to be determined by a parameter optimization procedure that minimizes or maximizes certain quality criteria adjoined to the system.

The method was applied to the determination of open loop commands for a STOL aircraft in the landing phase. The criteria of noise, fuel, time, and flight path deviation were considered as performance indexes.

The problem required the simultaneous time history optimization of three control variables – pitch angle, thrust angle, and throttle angle – under the influence of input, state, and terminal constraints. Three types of results were obtained:

1. Optimal controls for straight-line flight paths

2. Optimal controls and corresponding landing flight paths where only the design constraints of the aircraft and terminal conditions were considered

3. Optimal landing controls and trajectories of practical interest, in the sense that safety, comfort, and flight path constraints were added to the design constraints.

The first type of results indicated that, for a given flight path angle and speed, one should adjust the throttle angle to the lowest admissible value satisfying both the constraints of minimum throttle angle and maximum angle of attack, for both minimum noise and minimum fuel criteria. The trajectories obtained with only design and touchdown constraints show that for a *noise minimum* landing flight it is reasonable to fly at first as high as possible for as long as possible, then to descend with a minimum thrust amplitude and a maximum angle of attack, and finally to increase thrust for touchdown.

If *fuel consumption* is the optimization criterion, then the flight path trajectory shows an initial rapid descent requiring very little fuel. For the middle and last part of the flight a medium fuel rate is necessary to hold the altitude and meet the final conditions.

In contrast, the *time minimum* flight path trajectory displays a nearly straight-line shape. During the complete flight the thrust magnitude is high at first to accelerate the aircraft to the allowed speed limit and then to decelerate it, with thrust reversal, to an admissible touchdown speed. Another characteristic item of this flight is a negative pitch angle for the whole trajectory.

For trajectories involving safety, comfort, and flight path constraints, in addition to the touchdown and design constraints, it was concluded that: to decrease the average effective noise during a landing, the descent speed, angle of attack, glide slope, and touchdown speed should be held at the highest possible or highest admissible values. Because of the constraints imposed, the fuel and time required also tend to be reduced.

Ames Research Center
National Aeronautics and Space Administration
Moffett Field, Calif., 94035, June 1, 1972

APPENDIX A

FINDING AN EXTREMUM OF A BOUNDED MULTIVARIABLE FUNCTION WITHOUT DETERMINATION OF THE DERIVATIVES

The static optimization algorithm is explained here in more detail. (The corresponding Fortran-Subroutine EXTREM is displayed at the end of this appendix.) This algorithm is best suited for the search of a local extremum (maximum or minimum) of a multivariable function, the gradient of which is impossible or difficult to obtain directly (e.g., functional optimization or parameter optimization of a complex system). The function, which may be analytical or computed indirectly, can include any number of independent variables and any number of inequality constraints on them or functions of them. It is possible to change the boundaries during the optimization procedure.

METHOD

Basically, the algorithm for the search of the extremum of a bounded multivariable function has to perform the following tasks: (1) choose the directions of search, (2) determine the optimum along a line, (3) define the size of each search step, and (4) consider the boundaries limiting the search procedure.

Choice of Search Direction

The first main line (optimal search direction) is given by the user in form of an array DX(K), K being the number of variables. This array contains K properly scaled increments defining the initial step sizes along each variable about the guessed initial point $\vec{X}_i$, which is defined as a vector in an array X(K). Along this first line the approximately extremal point $\vec{X}_{i+1}$ is determined. After this first iteration a second line, going through $\vec{X}_{i+1}$ and being orthogonal to the main direction, is defined by a Gram-Schmidt orthogonalization process (fig. 26). Again the near-extremal point $\vec{X}_{i+2}$ along this secondary direction is determined (second iteration) and a third line is defined, if there are more than two coefficients, that passes through $\vec{X}_{i+2}$ and is orthogonal to the two first directions.

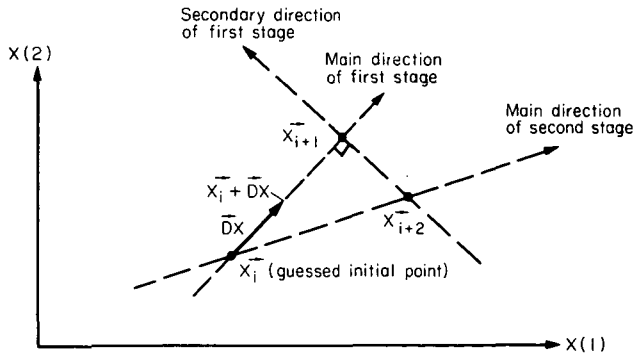

Figure 26.– Determination of the main search direction in the case of a two variable problem.

This procedure is repeated until the extremal point $\vec{X}_{i+k}$ along the Kth line, which is orthogonal to all previous directions, has been determined. Thus the first stage (K iterations) is accomplished. The new main direction for the

following stage is now given by the line going through the initial point $\vec{X}_i$ and the extremal point $\vec{X}_{i+k}$ of the last iteration of the previous stage. The procedure just described for the determination of the main and secondary search directions may begin again by setting $\vec{X}_i = \vec{X}_{i+k}$.

Determination of the Optimum Along a Line

To start, the function values, F_1 at $\vec{X}_1 - \vec{DX}$, F_2 at $\vec{X}_1$ and F_3 at $\vec{X}_1 + \vec{DX}$ are evaluated (search steps) and a parabolic extrapolation (or interpolation) is performed to find the extremum of a fictitious parabola going through the three defined points (extrapolation or interpolation step)

$$\vec{X}_{i+1} = \vec{X}_i + \frac{\vec{DX}}{|F_1 - 2F_2 + F_3|} \frac{F_3 - F_1}{2M_M}$$

where

$M_M = +1$ for the search of a maximum

$= -1$ for the search of a minimum

This equation is obtained by solving for the coefficients of a parabola at the three given values, then determining the position of $\vec{X}_{i+1}$ at the extremum of the parabola. In this formula the absolute value of $(F_1 - 2F_2 + F_3)$ is taken so that the new point $\vec{X}_{i+1}$ will be closer to the expected extremum than the old point $\vec{X}_i$ even if inflection points are located between the identified part of the curve and the extremum (see fig. 27).

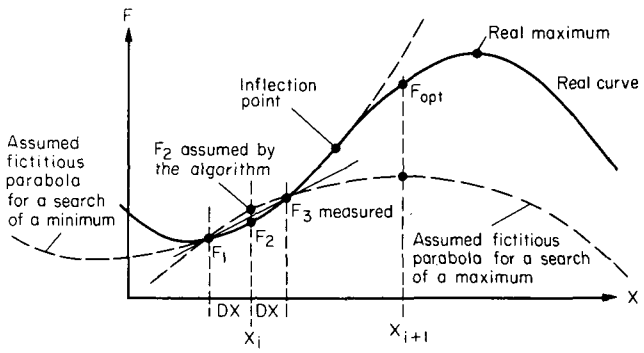

Figure 27.– One-dimensional case when an inflection point is located between the identified part of the curve and the extremum sought.

The algorithm limits the progression of the new point $\vec{X}_{i+1}$ with respect to a maximum of 20 step sizes $\vec{DX}$ (e.g., if $|F_1 - 2F_2 + F_3| = 0$). The function value F_{opt} at the new near-optimal point $\vec{X}_{i+1}$ along the line is evaluated, and these coordinates are taken as bases for the next iteration, even if F_{opt} is worse than F_2. However, if an undesirable difference between F_{opt} and F_2 is greater than four times the absolute value of the difference between the function values at the end of the last two iterations, the progression of the new point $\vec{X}_{i+1}$ is divided by two and another function value is evaluated. The same procedure is repeated until the above criterion for the transition to the next iteration along another line holds. Note that in some cases where the new point is allowed to have a slightly worse function value than the old point, the operating point leaves the bottoms of narrow valleys or the tops of sharp ridges, which is advantageous when these valleys or ridges present sharp corners.

Definition of Step Size

The different step sizes along each direction for the first stage are given by the array DX(K). If during any iteration the distance between the new point and the old is smaller than one quarter of

the current step size along this line, the current step size is divided by 4. If the new point is more than 20 times the current step size away from the old point, then the step size will be multiplied by 2.

By this procedure the search steps are allowed to decrease near the optimum or within tight curves and to increase again once these curves are passed.

Consideration of Boundaries

Before any function value is computed, the program given by the user is checked to determine if the current point lies within the permitted area. If this is not the case, the control is returned to the program EXTREM, which will deliver another point that satisfies the constraints. To compute a new point, if the previous one was outside the permissible area, the algorithm discerns two cases: (1) if the previous trial has been a *search step* as outlined in the preceding section, the step size is divided by 4 and the new point $\vec{X}_{i+1}$ will be placed at the other side of $\vec{X}_i$ away from the boundary (fig. 28, line A) and (2) if the previous trial has been an *extrapolation* or *interpolation step*, the progression of the new point $\vec{X}_{i+1}$ in the direction of the boundary will be divided by 10 (fig. 28, line B).

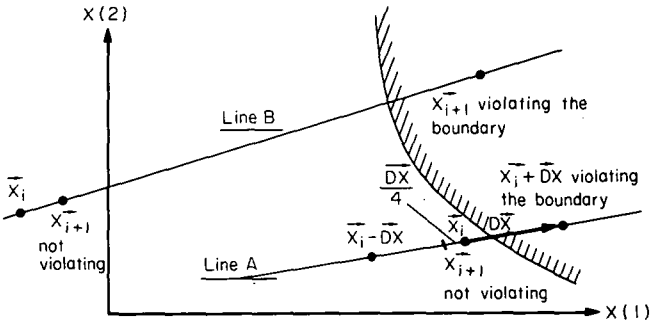

Figure 28.– Two-dimensional situation near a boundary.

Restrictions

The guessed initial vector, given by the user, should not lie outside the defined boundaries. Moreover, even though one may shift the limits defining the valid region while the operating point is converging to the extremum, current values of the variables (arguments) must not lie beyond the boundaries.

The stopping conditions (on the function value, the arguments, and the number of stages allowed to reach the optimum) should be sufficiently severe (small values for DFMAX and DXMAX, and a large number for LMAX) to avoid false convergence (e.g., stopping at sharp edges). This severeness is reasonable, especially when sharp edges exist. One must allow the step size to diminish sufficiently so that the optimization procedure, instead of stopping at the barriers, may follow the contour of the edges.

APPLICATION OF THE ALGORITHM

Calling Sequence

```
EXTERNAL
FN
DIMENSIØN X(...), DX(...), S(.....)
CALL EXTREM (FN, K, X, DX, S, DFMAX, DXMAX, LMAX, FØPT, IW)
```

with FN - name of subroutine supplied by user to determine if current arguments lie within the specified boundaries and, if yes, to evaluate the corresponding function value.

K - positive number whose magnitude is the number of independent variables of the function.

X - one-dimensional array whose K elements contain the initial guess arguments of the K independent variables. At the end of the optimization they deliver the final values of those arguments.

DX - one-dimensional array whose K elements define the K initial step sizes along each variable about the initially guessed point.

S - two-dimensional array defining the supplementary working space needed; it should be dimensioned (K, K + 3).

DFMAX - stopping condition on function variation; the optimization procedure stops if during the last stage the variation of the function value was smaller than DFMAX.

DXMAX - stopping condition on arguments; the optimization procedure stops if during the last stage the absolute variation of the argument vector was smaller than DXMAX.

LMAX - stopping condition on number of stages; the optimization procedure stops if the current number of stages is equal |LMAX|. The sign of LMAX indicates if a *maximum* is sought (positive sign) or a *minimum* (negative sign).

FØPT - function value at the end of the optimization procedure.

IW - Writing instructions:

±1 all outputs suppressed (e.g., results transferred to the user's main program).

±2 final outputs only

±3 outputs at the end of each stage

The sign of this instruction indicates if boundaries are involved (positive sign) or not (negative sign). Note that the optimization procedure stops if at least one of the three stopping conditions holds.

Form of the Output

```
STAGE NUMBER ...  TRIAL  NUMBER  ...  DL =

FU =              AR(1) =          DS(1) =
                  AR(2) =          DS(2) =
                    .                .
                    .                .
                    .                .
                  AR(K) =          DS(K) =
```

where

DL	= magnitude of the argument vector variation during the last stage
FU	= current function value
AR(1) . . . AR(K)	= current argument values (variables)
DS(1) . . . DS(K)	= step sizes in the main direction S(1) and in the orthogonal secondary directions S(2) . . . S(K)

The user must supply a subroutine for the determination of the function values. Any inequality constraints on the arguments or on functions of the arguments may be introduced in this subroutine by setting LI = LI + 1 (defined below) in the case that one or several of the current *arguments lie on the wrong side of the specified boundaries*. In this case a special instruction sends the flow back to the program EXTREM and the function value is not computed. New arguments are then determined by the program EXTREM, which do not violate the boundaries. This subroutine FN may have the following form:

```
SUBROUTINE  FN(AR, F, LI, N)
DIMENSIØN AR(1)
IF (LOGICAL EXPRESSION) LI = LI + 1 }
IF (LI.GT.1) RETURN                 } necessary only in the case that boundaries are involved
F = ...
N = N+1
RETURN
END
```

with:

LOGICAL EXPRESSION - should be true if one or several of the arguments lie in the forbidden area

F - function value corresponding to the current arguments

N - current number of trials (function evaluations)

The constraints may be changed at each trial; as noted, they can be a function of the current arguments AR(K) or even of the current function value F.

Storage Requirements

The program contains built-in variable dimensions so that its working space is defined by the calling program; the total vector argument storage needed (X, DX, and S vectors) is K*(K+5) for K independent variables and for any number of inequality constraints. The program itself comprises fewer than 100 instructions and takes 15A4 hexadecimal bytes of storage (double precision) for the Fortran G compiler of the OS.

EXAMPLES

The extrema of both analytic and computed functions have been determined with the described method. The optima-search results of five analytic functions are shown (computation in double precision) here. The first is Rosenbrock's curved valley (ref. 11):

$$F = 100(X_1^2 - X_2)^2 + (1 - X_1)^2 \tag{A1}$$

where

True min: $X_1 = X_2 = 1$, $F = 0$
Initial values: $X_1 = -1.2$, $X_2 = 1$
Initial step sizes: $DX_1 = 1$, $DX_2 = 1$

State after 102 trials (function evaluations): $X_1 = 0.9858$, $X_2 = 0.9718$, $F = 2.006 \times 10^{-4}$.

The second is a test function suggested by Aubrun (ref. 5), a steep, narrow, winding ridge with a horizontal inflection point along the top of this ridge:

$$F = -100(X_1^3 + X_1^2 - X_1 - X_2)^2 - (X_1^3 - 1)^2 \tag{A2}$$

where

True min: $X_1 = X_2 = 1$; horizontal inflection point $X_1 = X_2 = 0$
Initial point: $X_1 = -2.2$, $X_2 = -2$
Initial step sizes: $DX_1 = DX_2 = 1$

State after 368 trials: $X_1 = 1.0011$, $X_2 = 1.0046$, $F = 1.2237 \times 10^{-5}$.

The third is a linear function with discontinuities which cannot be approximated by a quadratic – given by R. F. Wheeling (ref. 12):

$$F = -3|X_1| - |X_2| \tag{A3}$$

where

Max: $X_1 = X_2 = 0$
Initial point: $X_1 = X_2 = 10$
Initial step sizes: $DX_1 = DX_2 = 1$

State after 129 trials: $X_1 = -7.8899 \times 10^{-5}$, $X_2 = -2.5147 \times 10^{-4}$, $F = -4.8817 \times 10^{-4}$.

The fourth is Rosenbrock's parcel problem where the maximum lies on three boundaries (ref. 11):

$$F = X_1 X_2 X_3 \qquad \text{with boundaries} \qquad \left.\begin{array}{l} 0 \leqslant X_1 \leqslant 20 \\ 0 \leqslant X_2 \leqslant 11 \\ 0 \leqslant X_1 + 2X_2 + 2X_3 \leqslant 72 \end{array}\right\} \qquad \text{(A4)}$$

where

Correct result: $X_1 = 20; X_2 = 11; X_3 = 15, F = 3{,}300$
Initial point: $X_1 = X_2 = X_3 = 10$
Initial step sizes: $DX_1 = DX_2 = DX_3 = 1$

State after 484 trials: $X_1 = 19.9999, X_2 = 10.9997, X_3 = 15.0001, F = 3{,}299.953$.

The fifth is Powell's fourth-power function, which cannot be approximated by a quadratic near the minimum (ref. 13):

$$F = (X_1 + 10X_2)^2 + 5(X_3 - X_4)^2 + (X_2 - 2X_3)^4 + 10(X_1 - X_4)^4 \qquad \text{(A5)}$$

where

Min $X_1 = X_2 = X_3 = X_4 = 0$
Initial point: $X_1 = 3; X_2 = -1; X_3 = 0; X_4 = 1$
Initial step sizes: $DX_1 = DX_2 = DX_3 = DX_4 = 1$

State after 181 trials: $X_1 = -9.7493 \times 10^{-3}$, $X_2 = 9.7492 \times 10^{-4}$, $X_3 = -3.7262 \times 10^{-3}$, $X_4 = -3.7280 \times 10^{-3}$, $F = 1.8205 \times 10^{-8}$.

Further reduction of F is very slow.

The program EXTREM has also been used to search the optimum of some bounded functionals (computed functions), such as the optimal trajectories of rockets and the STOL aircraft described in this report. The procedure was tried successfully on problems involving up to 30 parameters to be optimized.

FORTRAN PROGRAM

Despite its simplicity and relatively small size, the Fortran program given below finds the local minimum or maximum nearest a given initial point of any constrained analytical or computed multivariable function or functional. This algorithm is believed to be more efficient (in terms of the number of times the function must be evaluated to reach the extremum with a given precision) than other procedures described in the literature (ref. 14).

```
      SUBROUTINE EXTREM(F,K,X,DX,S,DFMAX,DXMAX,LMAX,FOPT,IW)                HGJ  01
C FINDING AN EXTREMUM OF A BOUNDED MULTIVARIABLE FUNCTION                   HGJ  02
C WITHOUT DETERMINATION OF THE DERIVATIVES                                  HGJ  03
C (SINGLE PRECISION PROGRAM)                                                HGJ  04
      DIMENSION X(1),DX(1),S(K,1)                                           HGJ  05
      L=0                                                                   HGJ  06
      LI=1                                                                  HGJ  07
      N=0                                                                   HGJ  08
      DO 1  I=1,K                                                           HGJ  09
      S(I,1)=X(I)                                                           HGJ  10
    1 S(I,2)=X(I)-DX(I)                                                     HGJ  11
      CALL F(X,F2,LI,N)                                                     HGJ  12
      FE=F2                                                                 HGJ  13
      IF(LI.GT.1)WRITE(6,2)                                                 HGJ  14
    2 FORMAT(1X,'INITIAL ARGUMENTS OUTSIDE BOUNDARIES')                     HGJ  15
    3 IF(KC.GE.K.OR.KC.LT.0.OR.L.EQ.0)KC=0                                  HGJ  16
      KC=KC+1                                                               HGJ  17
      S(1,3)=0.                                                             HGJ  18
      DO 4  I=1,K                                                           HGJ  19
      S(I,4)=S(I,1)-S(I,2)                                                  HGJ  20
    4 S(1,3)=S(1,3)+S(I,4)**2                                               HGJ  21
      S(1,3)= SQRT(S(1,3))                                                  HGJ S22
C     S(1,3)=DSQRT(S(1,3))                                                  HGJ D22
      IF(IABS(IW).GE.3)WRITE(6,23)L,N,S(1,3),F2,(I,X(I),I,DX(I),I=1,K)      HGJ  23
      IF(L.GE.IABS(LMAX).OR.S(1,3).LT.DXMAX.OR. ABS(FF-FOPT)                HGJ S24
C     IF(L.GE.IABS(LMAX).OR.S(1,3).LT.DXMAX.OR.DABS(FF-FOPT)                HGJ D24
     1.LT.DFMAX.AND.L.GT.0.OR.(LI.GT.1.AND.L.EQ.0))GOTO22                   HGJ  25
      IF(K.EQ.1)GOTO9                                                       HGJ  26
      DO 8  J=2,K                                                           HGJ  27
      KD=-2+J+KC                                                            HGJ  28
      IF(KD.GT.K)KD=KD-K                                                    HGJ  29
      S(J,3)=0.                                                             HGJ  30
      DO 7  I=1,K                                                           HGJ  31
      S(I,J+3)=0.                                                           HGJ  32
      IF(I.EQ.KD)S(I,J+3)=S(1,3)                                            HGJ  33
      JM=J-1                                                                HGJ  34
      DO 6  JK=1,JM                                                         HGJ  35
    6 S(I,J+3)=S(I,J+3)-S(KD,JK+3)*S(1,3)/S(JK,3)*S(I,JK+3)/S(JK,3)         HGJ  36
    7 S(J,3)=S(J,3)+S(I,J+3)**2                                             HGJ  37
      S(J,3)= SQRT(S(J,3))                                                  HGJ S38
C     S(J,3)=DSQRT(S(J,3))                                                  HGJ D38
      IF(S(J,3).LT.1.D-30)GOTO3                                             HGJ  39
    8 CONTINUE                                                              HGJ  40
    9 DO 10  I=1,K                                                          HGJ  41
   10 S(I,2)=S(I,1)                                                         HGJ  42
      L=L+1                                                                 HGJ  43
```

```
      FF=FOPT                                                          HGJ  44
      DO 21 M=1,K                                                      HGJ  45
      DO 11 I=1,K                                                      HGJ  46
   11 S(I,M+3)=S(I,M+3)/S(M,3)*DX(M)                                   HGJ  47
      IF(IW.GT.0)LI=3                                                  HGJ  48
   12 IF(IW.GT.0)LI=LI-1                                               HGJ  49
      LJ=LI                                                            HGJ  50
      DO 13 I=1,K                                                      HGJ  51
      X(I)=S(I,1)-S(I,M+3)                                             HGJ  52
   13 S(I,M+3)=S(I,1)-X(I)                                             HGJ  53
      CALL F(X,F1,LI,N)                                                HGJ  54
      BO=1.                                                            HGJ  55
   14 DO 15 I=1,K                                                      HGJ  56
      X(I)=S(I,1)+S(I,M+3)/BO                                          HGJ  57
   15 S(I,M+3)=X(I)-S(I,1)                                             HGJ  58
      IF( ABS(BO).GT.1.1)GOTO20                                        HGJ S59
C     IF(DABS(BO).GT.1.1)GOTO20                                        HGJ D59
      CALL F(X,F3,LJ,N)                                                HGJ  60
      IF(LI+LJ.EQ.4)GOTO12                                             HGJ  61
      IF(LJ.GT.2)BO=-4.                                                HGJ  62
      IF(LI.GT.2)BO=+4.                                                HGJ  63
      IF(LI.GT.2.OR.LJ.GT.2)GOTO14                                     HGJ  64
   16 ST=0.                                                            HGJ  65
      DO 18 I=1,K                                                      HGJ  66
      X(I)=S(I,1)                                                      HGJ  67
      IF( ABS(S(I,M+3)).LT.1.E-30)GOTO18                               HGJ S68
C     IF(DABS(S(I,M+3)).LT.1.D-30)GOTO18                               HGJ D68
      S(I,M+3)=S(I,M+3)/LI                                             HGJ  69
      IF( ABS(2.*F2-F1-F3).LT.1.E-30)GOTO18                            HGJ S70
C     IF(DABS(2.*F2-F1-F3).LT.1.D-30)GOTO18                            HGJ D70
      X(I)=S(I,1)+S(I,M+3 )/ ABS(F1-2.*F2+F3)*(F3-F1)/ISIGN(2,LMAX)    HGJ S71
C     X(I)=S(I,1)+S(I,M+3 )/DABS(F1-2.*F2+F3)*(F3-F1)/ISIGN(2,LMAX)    HGJ D71
   18 ST=ST+(X(I)-S(I,1))**2                                           HGJ  72
      IF(16.*ST.LT.DX(M)**2)DX(M)=DX(M)/4.                             HGJ  73
      IF(ST.LT.400.*DX(M)**2.AND. ABS(2.*F2-F1-F3).GE.1.E-30)GOTO20    HGJ S74
C     IF(ST.LT.400.*DX(M)**2.AND.DABS(2.*F2-F1-F3).GE.1.D-30)GOTO20    HGJ D74
      DO 19 I=1,K                                                      HGJ  75
      IF( ABS(S(I,M+3)).LT.1.E-30)GOTO19                               HGJ S76
C     IF(DABS(S(I,M+3)).LT.1.D-30)GOTO19                               HGJ D76
      X(I)=S(I,1)+ SIGN(S(I,M+3),(F3-F1)/S(I,M+3))*ISIGN(20,LMAX)      HGJ S77
C     X(I)=S(I,1)+DSIGN(S(I,M+3),(F3-F1)/S(I,M+3))*ISIGN(20,LMAX)      HGJ D77
   19 CONTINUE                                                         HGJ  78
      DX(M)=DX(M)*2.                                                   HGJ  79
   20 LI=+1                                                            HGJ  80
      BO=-BO                                                           HGJ  81
      IF( ABS(BO).GT.1.1)DX(M)=DX(M)/3.                                HGJ S82
```

```
C       IF(DABS(BO).GT.1.1)DX(M)=DX(M)/3.                                HGJ D82
        CALL F(X,FOPT,LI,N)                                              HGJ  83
        IF(LI.GT.1)LI=10                                                 HGJ  84
        IF(ISIGN(1,LMAX)*(FOPT-F2).LT.- ABS(FE-F2)*4..AND.LI.NE.10)LI=2  HGJ S85
C       IF(ISIGN(1,LMAX)*(FOPT-F2).LT.-DABS(FE-F2)*4..AND.LI.NE.10)LI=2  HGJ D85
        IF(LI.GT.1.AND. ABS(BO).GT.1.1)GOTO14                            HGJ S86
C       IF(LI.GT.1.AND.DABS(BO).GT.1.1)GOTO14                            HGJ D86
        IF(LI.GT.1)GOTO16                                                HGJ  87
        FE=F2                                                            HGJ  88
        F2=FOPT                                                          HGJ  89
        DO 21 I=1,K                                                      HGJ  90
   21   S(I,1)=X(I)                                                      HGJ  91
        GOTO3                                                            HGJ  92
   22   IF(IABS(IW).EQ.2)WRITE(6,23)L,N,S(1,3),F2,(I,X(I),I,DX(I),I=1,K) HGJ  93
   23   FORMAT(//1X,9HSTAGE NO.,I3,10X,9HTRIAL NO.,I6,12X,3HDL=E15.8,/1X, HGJ  94
       13HFU=E15.8,/(23X,3HAR(,I2,2H)=,E15.8,5X,3HDS(,I2,2H)=,E15.8))    HGJ  95
        RETURN                                                           HGJ  96
C THE LETTER D BEFORE THE IDENTIFICATION NUMBER MEANS DOUBLE PRECISION;  HGJ  97
C THE LETTER S SINGLE PRECISION.                                         HGJ  98
        END                                                              HGJ  99
```

REFERENCES

1. Pun, Lucas: Introduction to Optimization Practice. John Wiley and Sons, New York, 1969.

2. Beltrami, Edward J.: An Algorithmic Approach to Nonlinear Analysis and Optimization. Academic Press, New York, 1970.

3. Wick, Bradford H.; and Kuhn, Richard E.: Turbofan STOL Research at NASA. Astronaut. Aeronaut., vol. 9, no. 5, May 1971, pp. 32-50.

4. Quigley, H. C.; Sinclair, S. R. M.; Nark, T. C., Jr., and O'Keefe, J. V.: A Progress Report on the Development of an Augmentor Wing Jet STOL Research Aircraft. SAE Paper 710757, National Aeronautic and Space Engineering and Manufacturing Meeting, Los Angeles, Sept. 28–30, 1971.

5. Aubrun, Jean-Noël: Nonlinear Systems Identification in Presence of Nonuniqueness. NASA TN D–6467, 1971.

6. Meek, J. W.: What is STOL? Airline Pilot, vol. 39, Oct. 1970, pp. 8–10.

7. Ransone, R. K.: STOL Definition and Field Length Criteria. AIAA Paper 70–1240, 1970.

8. Lee, Robert; Farrell, James; Henry, George; and Lowe, Albert: Procedures for Estimating the Effects of Design and Operational Characteristics of Jet Aircraft on Ground Noise. NASA CR–1053, 1968.

9. Erzberger, Heinz; and Lee, Homer Q.: Technique for Calculating Optimum Takeoff and Climbout Trajectories for Noise Abatement. NASA TN D–5182, 1969.

10. Pearson, Karl S.: The Effects of Duration and Background Noise Level on Perceived Noisiness. FAA–ADS–78, April 1966.

11. Rosenbrock, H. H.: An Automatic Method of Finding the Greatest or Least Value of a Function. Computer J., vol. 3, no. 3, Oct. 1960, pp. 175–184.

12. Wheeling, R. F.: Optimizers: Their Structures. Commun. Assoc. Computing Machinery, vol. 3, no. 12, Dec. 1960, pp. 632-638.

13. Powell, M. J. D.: An Efficient Method for Finding the Minimum of a Function of Several Variables Without Calculating Derivatives. Computer J., vol. 7, no. 2, July 1964, pp. 155–162.

14. Pierre, Donald A.: Optimization Theory With Applications. John Wiley and Sons, New York, 1969, pp. 345–350.

NASA-Langley, 1972 — 2 A–4323

Page Intentionally Left Blank

"The aeronautical and space activities of the United States shall be conducted so as to contribute . . . to the expansion of human knowledge of phenomena in the atmosphere and space. The Administration shall provide for the widest practicable and appropriate dissemination of information concerning its activities and the results thereof."

— NATIONAL AERONAUTICS AND SPACE ACT OF 1958

NASA SCIENTIFIC AND TECHNICAL PUBLICATIONS

TECHNICAL REPORTS: Scientific and technical information considered important, complete, and a lasting contribution to existing knowledge.

TECHNICAL NOTES: Information less broad in scope but nevertheless of importance as a contribution to existing knowledge.

TECHNICAL MEMORANDUMS: Information receiving limited distribution because of preliminary data, security classification, or other reasons.

CONTRACTOR REPORTS: Scientific and technical information generated under a NASA contract or grant and considered an important contribution to existing knowledge.

TECHNICAL TRANSLATIONS: Information published in a foreign language considered to merit NASA distribution in English.

SPECIAL PUBLICATIONS: Information derived from or of value to NASA activities. Publications include conference proceedings, monographs, data compilations, handbooks, sourcebooks, and special bibliographies.

TECHNOLOGY UTILIZATION PUBLICATIONS: Information on technology used by NASA that may be of particular interest in commercial and other non-aerospace applications. Publications include Tech Briefs, Technology Utilization Reports and Technology Surveys.

Details on the availability of these publications may be obtained from:

SCIENTIFIC AND TECHNICAL INFORMATION OFFICE

NATIONAL AERONAUTICS AND SPACE ADMINISTRATION

Washington, D.C. 20546